Remote Sens. **2015**, *7*, 15082-15113; doi:10.3390/rs71115082

OPEN ACCESS

remote sensing

ISSN 2072-4292

www.mdpi.com/journal/remotesensing

Article

Estimation of CO_2 Sequestration by the Forests in Japan by Discriminating Precise Tree Age Category using Remote Sensing Techniques

Kotaro Iizuka [1,*] and Ryutaro Tateishi [2]

[1] Research Institute for Sustainable Humanosphere, Kyoto University, Gokasho, Uji, Kyoto 611-0011, Japan

[2] Center for Environmental Remote Sensing (CEReS), Chiba University, 1-33 Yayoi-cho, Inage-ku, Chiba 263-8522, Japan; E-Mail: tateishi@faculty.chiba-u.jp

***** Author to whom correspondence should be addressed; E-Mail: kotaro_iizuka@rish.kyoto-u.ac.jp; Tel.: +81-774-383-874.

Academic Editors: Guangxing Wang, Dengsheng Lu, Guomo Zhou, Conghe Song, Nicolas Baghdadi and Prasad S. Thenkabail

Received: 7 August 2015 / Accepted: 5 November 2015 / Published: 11 November 2015

Abstract: This study estimates CO_2 sequestration by forests in Japan using Land Remote Sensing Satellite (Landsat) Operational Land Imager (OLI) and the Advanced Land Observing Satellite (ALOS) Phased Array L-band Synthetic Aperture Radar (PALSAR) remote sensing data for the in-depth retrieval of forest growth stages (tree age). Landsat imagery was used to develop a detailed forest cover map, while the PALSAR data were used to estimate the volume information. The volume was converted to tree age information for each of the three forest types in Japan. An estimation of CO_2 sequestration values for each forest type and for each tree age from the forest inventory data was made. The forest cover map results in four classes, and the overall accuracy yields approximately 74%. For the volume estimation, Root Mean Square Error (RMSE) was computed with the ground reference information resulting in 105.58 m^3/ha. The final result showed that total CO_2 sequestration in Japan based on tree age forest subclasses yields 85.0 Mt·CO_2 (coniferous), 4.76 Mt·CO_2 (evergreen broadleaf) and 21.61 Mt·CO_2 (deciduous broadleaf), which in total is 111.27 Mt·CO_2. Using remote sensing techniques to quantitatively estimate CO_2 sequestration in Japanese forests has been shown both to have advantages and to offer further possibilities.

Keywords: forest; sequestration; CO_2; PALSAR; Landsat; tree age; Japan

1. Introduction

Forest resources are essential to life on Earth because forests play a large role in providing organic matter through photosynthesis, which is important for countless species of plants and animals, and in processing atmospheric gasses such as CO_2, which is of crucial environmental importance and among the most important issues faced in the 21st century: Global Warming/Climate Change. Research is performed and conferences are held to investigate this issue and its associated problems, and many nations are working together on policies to prevent or mitigate the associated problems and impacts [1,2]. Japan has been at the forefront of nations involved in the many activities related to this issue. The Kyoto Protocol and the Reducing emissions from deforestation and forest degradation mechanisms (REDD, REDD+) provided a new approach to finding solutions, giving the role of forests more importance, especially when focusing on how forests function as a carbon sink. Forest carbon sinks are highly important in the current research context, as 67% of the land in Japan is covered by forests [3]. Japan considers forests to be the top candidate for its CO_2 reduction process [4]. Prefectural Governments and private companies in Japan highly value forest carbon sequestration research; however, some Prefectures have not yet been involved in such processes even when they have a great amount of forest cover [5], which may be because they lack the equipment or effective methodology to quantitatively estimate carbon sequestration.

The estimation implemented in Japan mostly focuses on identifying forests as either natural or planted. Hiroshima and Nakajima [6] focused on the potential carbon sinks in Japanese plantation forests during the first commitment period of the Kyoto Protocol. They estimated that planted forests were expected to sequester 8.16–8.87 Mt·C/yr, depending on various scenarios of forest management based on silvicultural practices, and employed subsidies and forest workers' wages as predictor variables. Sasaki and Kim [7] estimated potential CO_2 sequestration by forests in Japan and the eligible sequestration under the condition of the Marrakesh Accords. Using the land use model and the carbon stock growth model, it has been estimated that the forests in Japan are likely to sequester 20.1 Mt·C/yr (planted forests: 15.3 Mt·C/yr, natural: 4.8 Mt·C/yr), and under the conditions of the Marrakesh Accords, it is estimated at 10.2 Mt·C/yr (planted forests: 7.3 Mt·C/yr, natural: 2.9 Mt·C/yr). Recently, the National Institute for Environmental Studies (NIES) Center for Global Environmental Research (CGER) calculated a result for the IPCC reports on the issue of forest carbon sinks, estimating the CO_2 sequestration by the forests of Japan [8]. Using the forest registration data from each prefectural government, and differentiating the forests by tree species, they have calculated the total CO_2 amount sequestered both aboveground and in litter and soil. Their results showed an estimate of 77.67 Mt·CO_2 for the year 2012.

Utilizing satellite remote sensing data for quantitative C/CO_2 estimations is challenging but well-known method for improving broad scale estimations compared to conventional ground-based observations [9]. The techniques can be separated into two major methodologies. The first is the indirect measure of C/CO_2, which calculates several parameters related to the function of the forest system, such as Leaf

Area Index (LAI), Photosynthetically Active Radiation (PAR) and others, and then models multiple parameters to estimate either Gross Primary Product (GPP) or Net Primary Product (NPP) [10,11]. The second method integrates detailed land cover information with ground observations of forest inventories [5]. Alternatively, both methods may be integrated together [12]. All these methods have advantages and disadvantages. For example, one popular product by the former method is the Moderate Resolution Imaging Spectroradiometer (MODIS) NPP [13], which can be collected globally with a fine temporal resolution. Depending on the need, such products can be unsatisfying because the spatial resolution of 1 km by 1 km is too coarse; when we want to focus more on a regional-scale analysis, a spatial resolution of 1 km cannot delineate the actual local environment accurately. The latter method is usually implemented in a regional scale analysis using fine resolution imagery, such as Landsat, to discriminate details in land cover/land use types to estimate accurate values for C/CO_2 content. This can also be conducted by indirectly estimating modeling parameters, but it is often performed with the associated forest inventory data collected from other ground observation sources and then integrated with the land cover information for the estimation. In comparison with MODIS, Landsat provides a much finer spatial resolution (30 m), making it possible to allocate the heterogeneity of the natural environment; however, there are again issues that must always be faced, such as the fundamental problem of utilizing optical imagery due to cloud cover. Fine resolution imagery has lower temporal resolution, and it is sometimes difficult to collect cloud free imagery through only a few observations. Sanga-Ngoie *et al.* [5] has utilized synthetic aperture radar (SAR) data to extract the forest parameters related to CO_2 sequestration. This method has shown the usefulness of implementing SAR to observe forest extent, which could be broadly usable in conditions where there is frequent cloud cover over the area of interest. This method made it clear that not only land cover type discrimination, but also tree age, or the growth stages of the forests, plays an important role. Taking these variables into account provides more accurate estimations for the overall result, because each forest growth stage differs in its sequestration rate [5,14]. Utilizing both optical and microwave satellite imagery makes this possible.

Most forest carbon sequestration capacity estimates within Japan are performed at a national scale, and detailed analyses at a regional scale are still rare; therefore, such estimates are either rough estimations on a national scale or detailed analysis on a local scale. Unfortunately, local-scale studies cannot be expanded to a national scale; they are only for smaller regions and do not apply to the country as a whole. The studies mentioned usually use a methodology involving a modeling base, site observation and statistics. However, detecting and locating forest resources does not take place. Locating precise forest resources of both forest types and their growth stages requires not only consideration of realistic estimation of sequestration [5,10,14–16] but also an understanding of the current status of the forest resources, which may be the most important information to gather for long-term sustainable plans to manage forests in a strategic way. Consequently, the objective of this research is to reassess the estimation of CO_2 sequestration (*i.e.*, NPP) by forest cover in Japan based on a precise evaluation of forest extent by both forest type and age, together with the use of remote sensing data, to quantitatively estimate the CO_2 sequestration potential.

2. Study Area

Our area of study focuses on mainland Japan (except Okinawa and small islands) (Figure 1). Japan is made up of over 7000 contiguous islands from the northeast to the southwest, with a total length of approximately 3000 km. Total land area is approximately 377,900 km^2. Over 60% of the land is recognized as mountainous (over 2000 m in altitude) and 12% as hilly. The total forested area makes up approximately 67% [3], the majority of which is located around the aforementioned mountain or hill areas. Climatic conditions in Japan vary widely due to its geographical location; its lands stretch from a southern latitude of 30 °N (Okinawa omitted) to a northern latitude of 45 °N. This range, together with the ocean currents, gives each region a different climate. Because of the variety in topography and climatic conditions, Japan has a great diversity of vegetation both horizontally and vertically. For example, there are over 6000 species of Pteridophytes, each of which has evolved and adapted to its specific location [17]. The dominant coniferous tree types in Japan are the Japanese cedar (*Cryptomeria japonica*) and cypress (*Chamaecyparis obtusa*) trees, which occur widely from the north to the south. As a whole, coniferous and broadleaf forests are distributed in approximately a 50/50 ratio, while 80% of coniferous forests tend to be planted forests that were part of a large plantation plan that lasted from the 1950s to the 1970s. On the other hand, the broadleaf forests are primarily natural (over 90%), and few deciduous or evergreen broadleaf trees have been planted. Broadleaf hardwoods are dominant in the central region, while mixed deciduous evergreen forests or evergreen broadleaf forests can be observed in the temperate south zones.

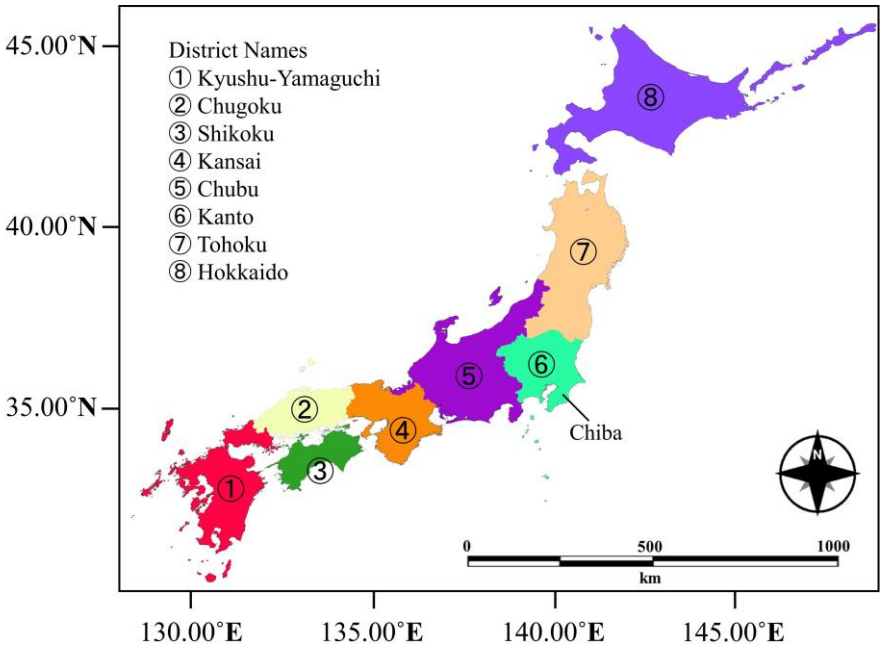

Figure 1. Study Area, Japan and its eight major districts.

Remote sensing data for Chiba Prefecture was used for a detailed analysis of statistical data, so a brief explanation is given. Chiba is located on the east coast of Japan along the Pacific Ocean, just east of the Tokyo metropolitan area, where the peninsula juts out. Climatic conditions include a warm oceanic climate, which is a condition with high humidity and high precipitation in summer, and low humidity and low precipitation in the winter. However, comparing the southern and northeastern regions of Chiba,

the climate is warm throughout the year in contrast to the inland area, which shows more diversity such as larger temperature drops in the winter [18]. Annual precipitation is highest in the southern area, with more than 2000 mm, and is next highest in the northern area, which has approximately 1400 mm to 1600 mm. The difference in precipitation clearly shows the distribution of the forests, which are more dense in the south and sparse in the north [18]. A characteristic of Chiba is that it is one of the flattest regions in Japan; the average land altitude is 46 m above sea level, and there are no mountains higher than 500 m in altitude.

3. Methods and Data

The overall flowchart of the methodology is shown in Figure 2. A three-step process is used: (1). Estimating the volume of the forests in Japan using SAR and converting these data to tree age information data; (2). Developing a detailed land cover (forest cover) map to allocate the precise forest types across the land area of Japan; and (3). Utilizing the obtained data from the preceding steps together with the CO_2 sequestration rate per unit area to estimate the sequestration values by each forest type and age.

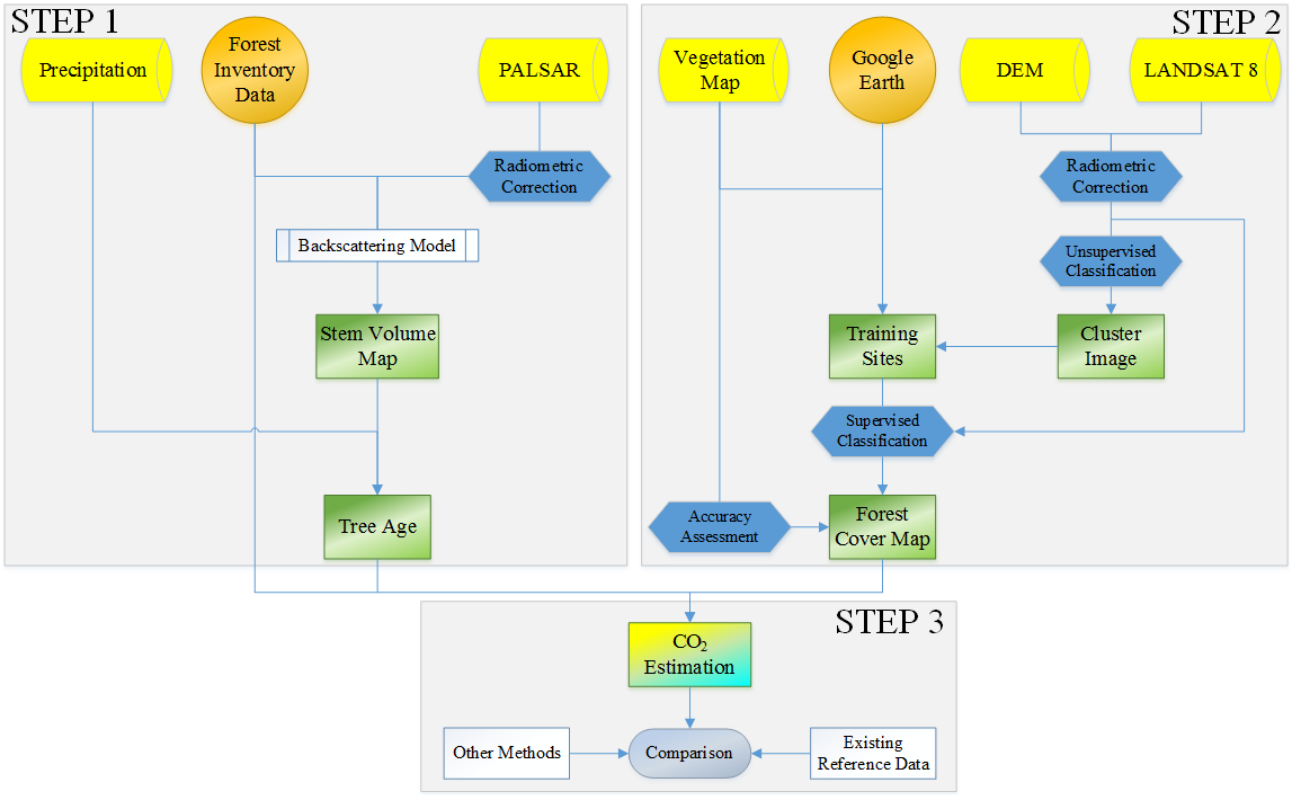

Figure 2. Overall flowchart of the methodology.

3.1. L-Band PALSAR for Volume Mapping

In the first step of the study, a simple relationship analysis was performed between the biophysical parameters collected from field observations by the Chiba Prefectural Government and the L-band backscattering intensity data collected by the Advanced Land Observing Satellite (ALOS) Phased Array L-band Synthetic Aperture Radar (PALSAR) provided by the Japan Aerospace Exploration Agency (JAXA). This step involved extracting the biophysical parameters (volumes) of the forested areas and

mapping them for the whole of Japan. The use of SAR for detecting forest parameters works because the radar waves are longer than the optical waves, so the radar beam penetrates through the top layer of canopy and scatters from the stems and branches of the trees when using L-band radar [19–23]. A number of studies have been conducted to develop models related to those studies' specific regions of interest. Those studies confirm that the backscattering signature correlates with forest parameters and that SAR images can be used to extract information related to forest biomass. While most of the papers present and acknowledge the possibility of extracting forest parameters using the L-band SAR information, some studies show difficulties in data interpretation [24], mostly due to distortions caused by local topography, which is also one of the challenges for this work.

To meet this topography challenge for the analysis, Chiba Prefecture was selected due to its relatively flat terrain, which limits this critical and fundamental topography problem when utilizing SAR imagery [25].

The 25 m PALSAR Global Mosaic (PGM) image used in this study was converted from the provided Digital Number (DN) values to the backscattering intensity information, also known as backscattering coefficients, using Equation (1). The PALSAR specification is in ascending Fine Beam Dual (FB) mode characterized by a 34.3 degree of off-nadir angle, calculated as:

$$\sigma^0 = 10 \times \log_{10}(\mathrm{DN}^2) + \mathrm{CF} \quad (1)$$

where σ^0 is the backscattering intensity represented in decibel units (dB) and CF is the calibration factor for the data obtained, depending on the observation period and polarization [26]. The image is already processed for ortho-rectification and slope correction [27], so further analysis uses these data directly without any additional correction.

A statistical analysis for formulating relationships among the field observation data of the forest stand characteristics and the remotely sensed microwave satellite data was carried out. The process analyzes the relationships between SAR backscattering intensity (σ^0) and the stand characteristics (volume) for the 25 m pixel spacing PALSAR image. The PALSAR image used here is the mean value of the years 2009 and 2010, to minimize local variations from such things as precipitation. Using the vegetation continuous field data [14], the sample plots were selected from an area of less than 70% forest cover to avoid uncertainties associated with scattering, as Iizuka and Tateishi [28] explain that attenuation of the radar beam is caused by high dense forested areas, resulting in lower backscattering values compared to the peak areas (70%–75% forest cover), and causing difficulties when interpreting the actual forest trend.

Using the result, the model function was applied to the 50 m PALSAR mosaic product (which can be downloaded free from the JAXA web page [29]) to obtain volume information for the forests across Japan. The 50 m PALSAR data were selected because of the spatial coverage and availability (it is freely available and covers the whole of Japan). The equation obtained from the relationship analysis was assumed to be acceptable to apply to the downscaled data, because several papers confirm an increase in accuracy and higher correlations when the pixel spacing is reduced [30,31].

DN values of the data from 2007 and 2009 were averaged to avoid small changes from backscattering caused by local environmental factors at that particular observation time (e.g., precipitation) and then converted to dB units. The data were then slope corrected, because they had been previously ortho-rectified but not slope corrected, resulting in enhancements of the backscatter from the rugged hills facing towards the sensor direction [28].

A correction method proposed by Zhou *et al.* [32] was modified and applied to the 50 m PALSAR mosaic product. The correction of the SAR imagery is performed by applying a slope correction factor to the original SAR data. The equation for the correction is as follows:

$$\sigma_c^0 = SCF^q \times \sigma^0 \quad (2)$$

where σ^0_c is the corrected sigma naught backscattering value, σ^0 is the original sigma naught backscattering data, q is the diffuse scattering, which is polarization dependent, and *SCF* is the slope correction factor for the correction of the topography, expressed as:

$$SCF = \frac{\cos i}{\sqrt{1 + \left(\frac{\tan a \times \sin a \times \sin 2\beta}{2}\right)^2}} \quad (3)$$

where cos *i* is the cosine of the incidence angle, α is the slope and β is the aspect. The HV polarization image of PALSAR was corrected using this method. The value for the diffuse scattering depends on the environment and was unknown in this case due to the large study area with differing forest structures, so here it has been assumed that q = 1. The volume map for the whole of Japan was obtained by applying the volume model equation to the corrected 50 m PALSAR mosaic product.

3.2. Land Cover Mapping of Japan

We selected and analyzed 35 scenes from the Land Remote Sensing Satellite (Landsat) Operational Land Imager (OLI) data published by the United States Geological Survey (USGS) to develop a land cover map of Japan that takes forest types into account. Each scene was processed with an Integrated Radiometric Correction [33] method to reduce effects from the atmosphere and topography, resulting in fewer errors throughout the classification process. Landsat OLI 5 bands (bands 2–6) along with the Normalized Difference Vegetation Index (NDVI), Normalized Difference Water Index (NDWI) [34], and Green Red Vegetation Index (GRVI) [35] were used to perform the supervised classification using a maximum likelihood algorithm. This yielded a final land cover product with 12 classes. However, our interests here are in the forest classes only, so the number of classes was reorganized into three forest type classes (coniferous, deciduous broadleaf, and evergreen broadleaf) plus one additional class (others), resulting in a total of four classes. These were utilized for further procedures along with the accuracy assessment, which is fundamental for evaluating the resulting categorical map [36]. The date of the acquired scenes included two from March, four from April, four from May, six from June, five from August, five from September and nine from October. Selection of the images was made by considering a general and critical issue for such optical images: that they were cloud-free. Not all scenes were completely cloud free. In such cases, selections were made from the clearest images that could be found. The specifications of the chosen data are listed in Table 1.

Table 1. Specification of the Landsat Imagery used.

Landsat OLI Data Sets				Landsat OLI Data Sets			
Region	**Path**	**Row**	**Date**	**Region**	**Path**	**Row**	**Date**
Kyushu Yamaguchi	112	36	2 May 2014	Tohoku	106	33	8 May 2014
	112	37	13 April 2013		107	31	29 April 2014
	112	38	13 April 2013		107	32	19 October 2013
	113	37	23 April 2014		107	33	17 September 2013
	113	38	29 October 2013		108	31	20 April 2014
Chugoku Shikoku Kansai	110	36	17 March 2014		108	32	4 June 2013
	110	37	17 March 2014		108	33	4 June 2014
	111	35	24 May 2013		108	34	4 June 2014
	111	36	24 May 2013	Hokkaido	105	30	2 June 2014
	111	37	11 May 2014		106	29	25 June 2014
	112	35	19 August 2013		106	30	25 June 2014
Chubu	108	35	7 August 2013		106	31	28 October 2013
	108	36	7 August 2013		107	29	19 October 2013
	109	35	14 August 2013		107	30	19 October 2013
	109	36	14 August 2013		108	28	10 October 2013
	109	37	17 October 2013		108	29	10 October 2013
	110	35	17 May 2013		108	30	10 October 2013
Kanto	107	34	17 September 2013				
	107	35	17 September 2013				
	107	36	17 September 2013				
	109	34	14 August 2013				

3.3. Estimating CO_2 Sequestration from the Forests of Japan

Estimation of the sequestration from Japanese forests was obtained by utilizing the two data sets described above (*i.e.*, the volume map and land cover map), along with an additional data set of forest inventory data provided by two Prefectural Governments and the precipitation data published by the Ministry of Land, Infrastructure, Transport and Tourism (MLIT) of Japan. CO_2 sequestration per unit area data published by the Tochigi Prefectural Government was used to estimate the sequestration values not only for each forest type but also for each tree age. This was achieved by transforming the volume map into ages among the different forest types, referring to the volume-tree age relationship data provided by the Oita Prefectural Government. The precipitation data were also used to help discriminate between growth rates for each region, which is an important step, because even with the same stem volume, the forests' per unit areas could have different tree ages due to local site productivity [37].

The stem volume-age relationship data provided by the Oita Prefectural Government is based on observations made on ground-level plots at multiple sites within Oita Prefecture. The curves were averaged for each growth region and computed as high, moderate and low growth rate areas. Each location within the study area that lies on a matching growth-rate region was determined to have a particular growth curve for that forest; the tree age conversion is based on that curve. To differentiate the growth rate of the study area, a relationship analysis was made using the precipitation data along with the total volume of growth made between the two periods of time. The sugi (cedar) and kunugi

(sawtooth oak) data were used as representative of the coniferous and deciduous broadleaf forests, respectively. Unfortunately, there is a lack of data for the evergreen broadleaf forests, so the growth rate is considered only for the first two classes. Here, the precipitation data were used to determine whether precipitation would be one of the limiting factors for forest growth.

The sequestration values were modified from the reference data published by the Tochigi Prefectural Government by taking a mean value of each tree type at each tree age range for deciduous and evergreen broadleaf forests, using the tree data for sawtooth oak, Japanese beech, Japanese zelkova and hornbeam for deciduous broadleaf forests, and using evergreen oak and chinquapin oak for the evergreen broadleaf forests. For the coniferous forests, a weighted mean value of the sugi (cedar) and hinoki (cypress) trees was taken as 7:3 because the distribution of those trees approximates that ratio for the whole of Japan. Together with the estimation, an in-depth analysis of the uncertainties of the estimated results was assessed by considering possible errors that could generate inaccuracies in the results.

4. Results

4.1. Stem Volume Modeling and Mapping

Figure 3 shows the trends of the stem volume *vs.* the backscattering intensity (dB) for both HH and HV polarizations. An increasing trend can be observed with the increasing parameter and increasing backscattering intensity, which is consistent with many of the other related studies [19–23,30,31]. According to these results, a second polynomial function from the HV polarization was selected and applied to obtain the stem volume information for the whole of Japan, because it has higher correlation compared to HH (HH: $R^2 = 0.2123$, HV: $R^2 = 0.2198$).

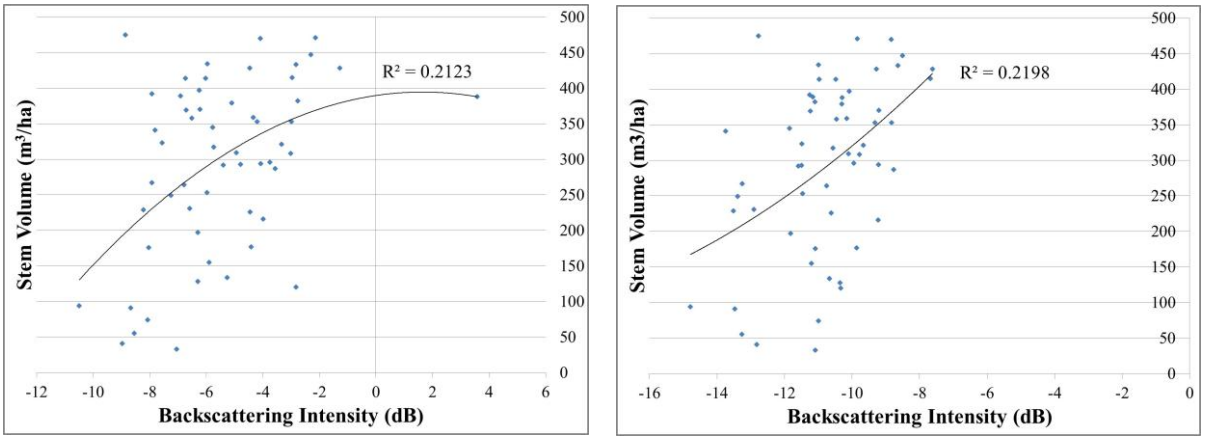

Figure 3. Relationship between Stem Volume (m^3/ha) and backscattering for HH (**left**) and HV (**right**) polarization at mean 25 m pixel spacing data from 2009 and 2010 (HH: $R^2 = 0.2123$, HV: $R^2 = 0.2198$).

The equation of the function is described as:

$$V = 1.4192\sigma_{HV}^{0^2} + 60.472\sigma_{HV}^{0} + 773.8 \quad (4)$$

where V is the stem volume and σ^0_{HV} is the backscattering intensity from the HV polarization. Validation of the backscattering model was assessed by using the remaining observation plot data that were not

used in the modeling process. Using the plot data as ground truth information, the root mean square error (RMSE) between the estimated results and the reference data was calculated. The RMSE result is 105.58 m^3/ha, and R^2 = 0.164 as shown in Figure 4. This model will be applied to obtain the stem volume information for the forested areas within Japan.

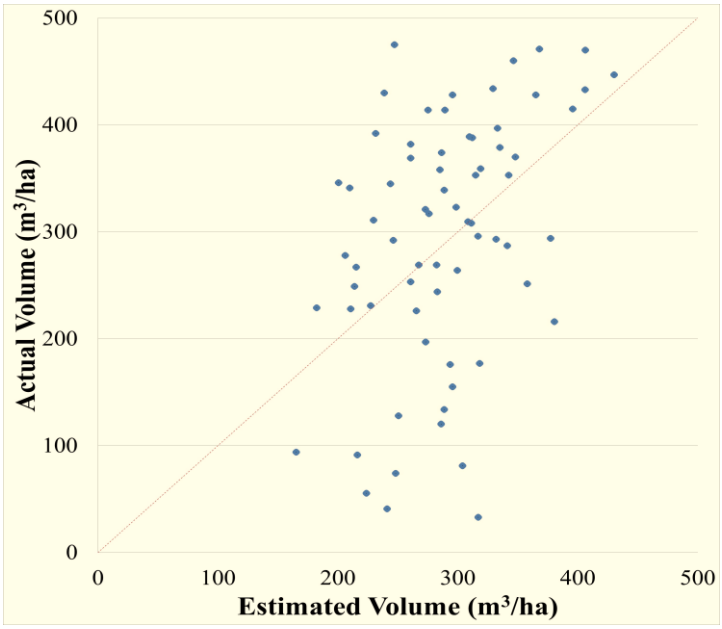

Figure 4. Validation of the backscattering model. The X-axis is the estimated volume (m^3/ha) using the model, and the Y-axis is the reference data from the observation plot. R^2 = 0.164 Root Mean Square Error (RMSE) = 105.58 m^3/ha.

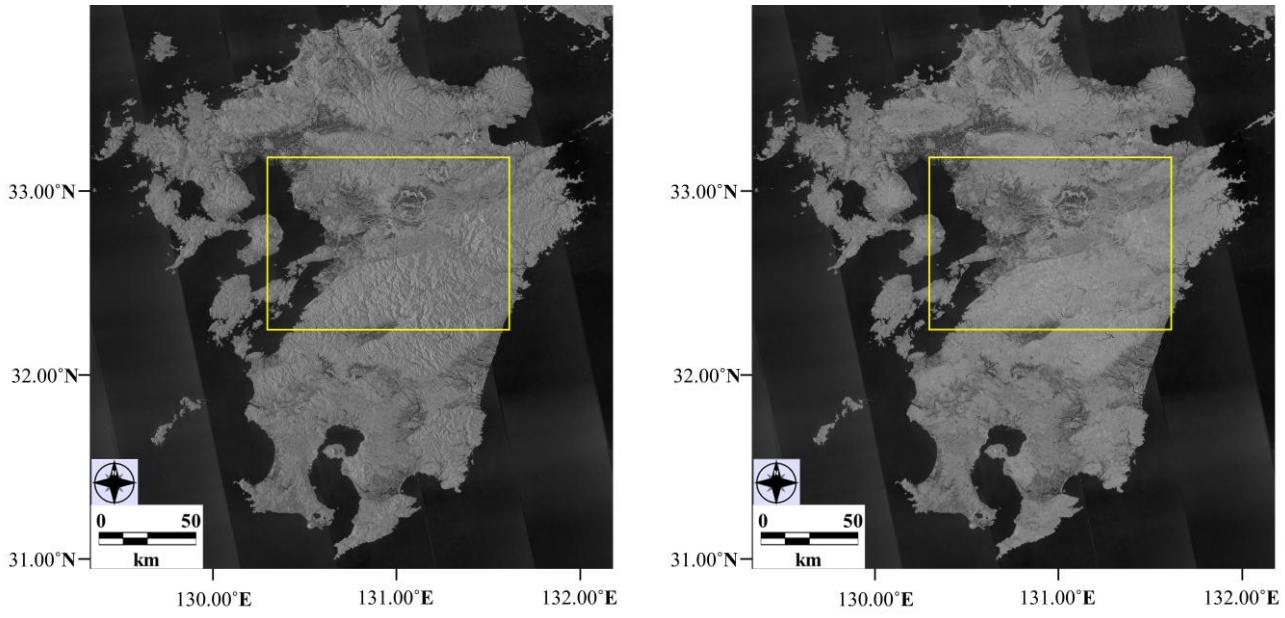

Figure 5. *Cont.*

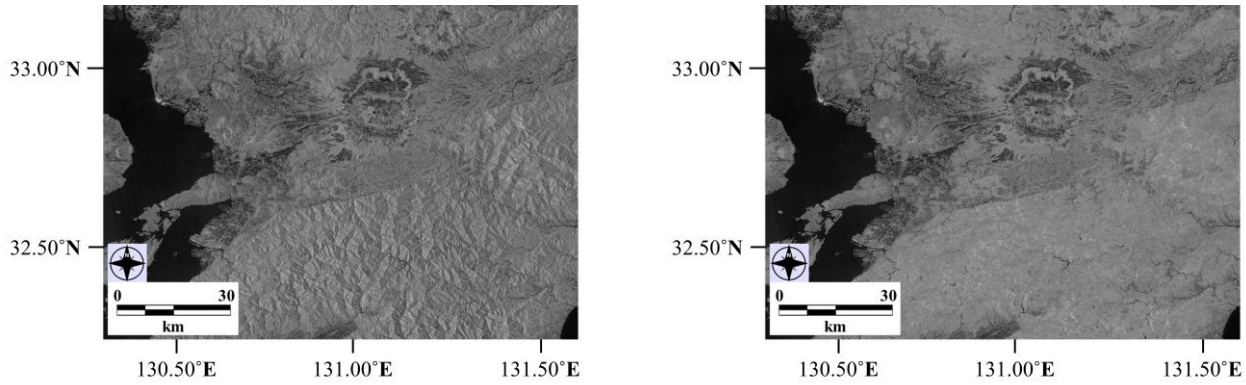

(**c**) (**d**)

Figure 5. Visual interpretation of the Phased Array L-band Synthetic Aperture Radar (PALSAR) 50 m at the Kyushu Island region, for (**a**) the original image and (**b**) the slope-corrected image of the HV polarization data. The (**c**,**d**) images show the zoomed areas from the (a,b) images, respectively.

Figure 5 shows the interpretation of the original and the corrected imagery of the PALSAR data. In addition to the interpretation, a quantitative evaluation of the performance of the correction was conductedby assessing the non-correlation between cos *i* and the corrected data. Comparing the correlation coefficients, the value shows r = 0.4 and r = 0.06 for non-corrected and corrected images, respectively. From these results, it is presumed that the correction of the PALSAR was performed successfully.

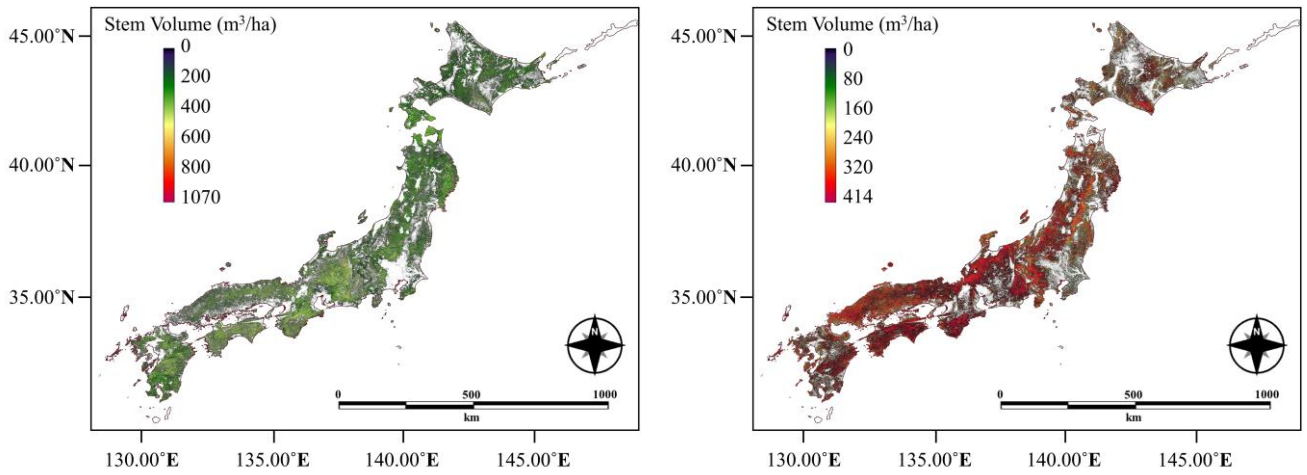

(**a**) (**b**)

Figure 6. Stem volume map of Japan for the (**a**) coniferous forests and (**b**) deciduous and evergreen broadleaf forests. Forest cover data were overlaid with the stem volume map to extract only the forest types needed for each stem volume map.

The formula (Equation (4)) obtained through the model was applied to the corrected PALSAR imagery to obtain stem volume information for the entire forest area of Japan. By doing this, the spatial distribution of the estimated stand volume for Japanese forests can be shown. However, this model is specific to the coniferous stands in Japan, and the possibility that backscattering characteristics of different forest types would give different trends due to the structure of the stand and leaf size should be

taken into account. Instead, for the broadleaf forests, a polynomial model developed by Wijaya [38] from the evergreen trees of Indonesia was applied to fit the situation (Equation (5)). Utilizing the two different models specific to those forest types, the stem volume distribution across Japan was obtained, as seen in Figure 6a,b. Using the model developed from the results of this study, the maximum stand volume of the coniferous forests reaches up to 1069 m^3/ha; for the broadleaf forests, it reaches up to 414 m^3/ha. Although the coniferous stand volume gives a high maximum value, most of the distributed areas lie near the 400–500 m^3/ha range and rarely exceeds 700 m^3/ha. The original stem volume information was distributed over all land cover types, so the exact location of each forest was extracted using the land cover map. The white areas in Figure 6 indicate non-coniferous (a) and non-broadleaf forests (b) areas.

$$V = 256.85 - (65.458\sigma^0) - (6.8\sigma^{0^2}) \quad (5)$$

4.2. Land Cover Map and Its Accuracy

The Landsat OLI images captured on multiple dates from years 2013 to 2014 were classified into the following 12 land cover types: water bodies, urban, paddy fields, crop lands, orchards, grasslands, silver grass, bare lands, coniferous forests, evergreen broadleaf forests, deciduous broadleaf forests and snow/clouds. These detailed classes were then reclassified into the three general forest classes and one other-than-forest class, resulting in a total of four land cover categories. Only the forest categories are of interest; the accuracy assessment was also performed with this map. The final product of the land cover map (before reclassification) of Japan is shown in Figure 7.

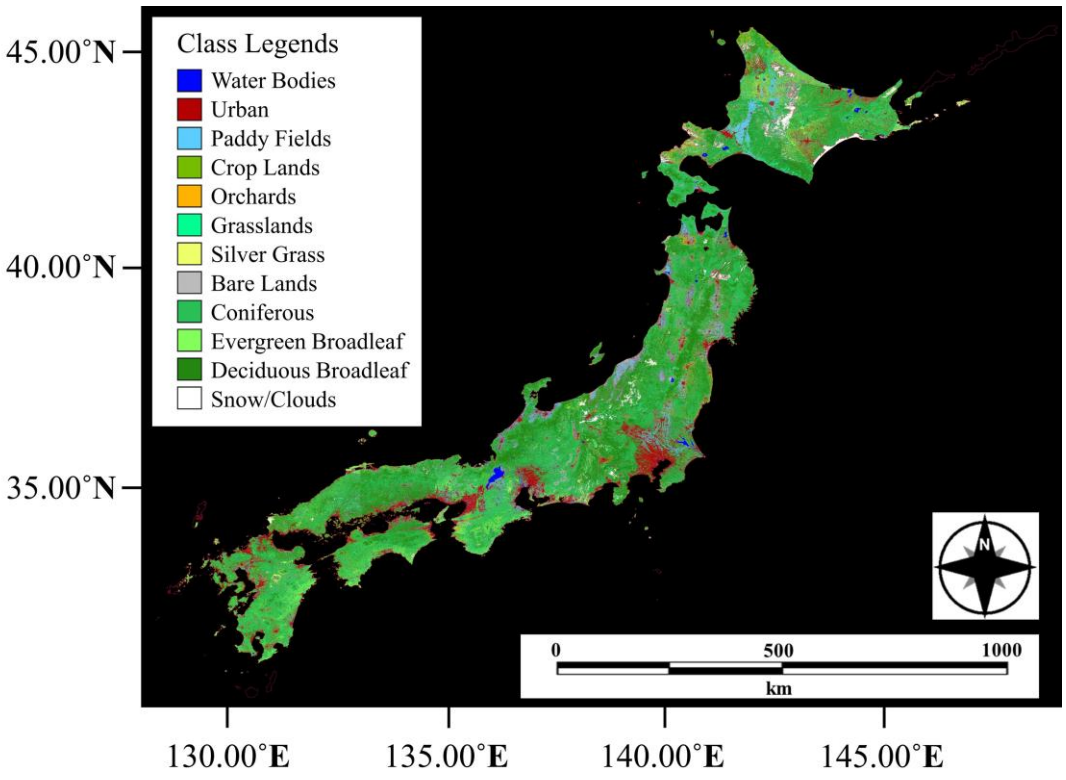

Figure 7. Land Cover map of Japan developed using 35 Landsat Operational Land Imager (OLI) scenes yielding 12 classes in total.

The ground truth points obtained from Google Earth together with the reference vegetation map [39] were used in the resulting land cover map to perform an accuracy assessment by outputting an error matrix (Table 2). The final number of ground truth points yields 3550 points. However, the number of points was normalized for each class to 1000 points, to make calculations and interpretation easier in the accuracy assessment. The overall accuracy of the land cover (forest cover) map result was 73.93%, and the overall Kappa Index of Agreement (KIA) result was 0.65. KIA is a statistical measure adapted for accuracy assessment in the remote sensing fields by Congalton and Mead [40]. KIA values range from 0 to 1, with zero representing completely random chance and 1 meaning a perfectly true agreement. In this study, KIA = 0.65, which could be said to show that the map is 65% likely to be the result of true agreement.

Table 2. Error Matrix showing the reference data (ground truth) *versus* the image classification. Overall accuracy shows approximately 74% and Kappa Index of Agreement (KIA) as 0.65.

KIA = 0.65		**Reference**					
		Coniferous	**Evergreen Broadleaf**	**Deciduous Broadleaf**	**Others**	**Total**	**ErrorC**
Classified	Coniferous	**852**	253	149	24	1278	0.3334
	Evergreen Broadleaf	41	**533**	113	30	717	0.2566
	Deciduous Broadleaf	59	200	**680**	54	993	0.3152
	Others	48	14	58	**892**	1012	0.1186
	Total	1000	1000	1000	1000	4000	
	ErrorO	0.1480	0.4670	0.3200	0.1080		0.2607

4.3. CO_2 Sequestration

4.3.1. CO_2 Sequestration by Forest Types and Ages

The stem volume-age relationship data were modified from the original Oita data [5] to compute high, moderate and low growth curves for coniferous and deciduous broadleaf forests (Figure 8), which were used in turn to convert the so-obtained stem volume map (Figure 6) into tree age classes. Figure 9 shows the analysis between annual precipitation and tree growth for coniferous and deciduous broadleaf forests.

The results show a clear trend in the relationship between precipitation and tree growth. For the sugi trees (coniferous), increasing precipitation results in larger tree growth. On the other hand, for the sawtooth oak (deciduous broadleaf), the opposite trend can be observed, where tree growth increases with decreasing precipitation. The negative trends in the deciduous broadleaf forests might be caused by the precipitation data used. The precipitation data are an annual value, which means that it was not taken into account during the time when deciduous trees are likely to be photosynthesizing. If the precipitation falls mostly in the fall or winter, the trees may not be able to take advantage of it and thus would have lower than expected growth rates.

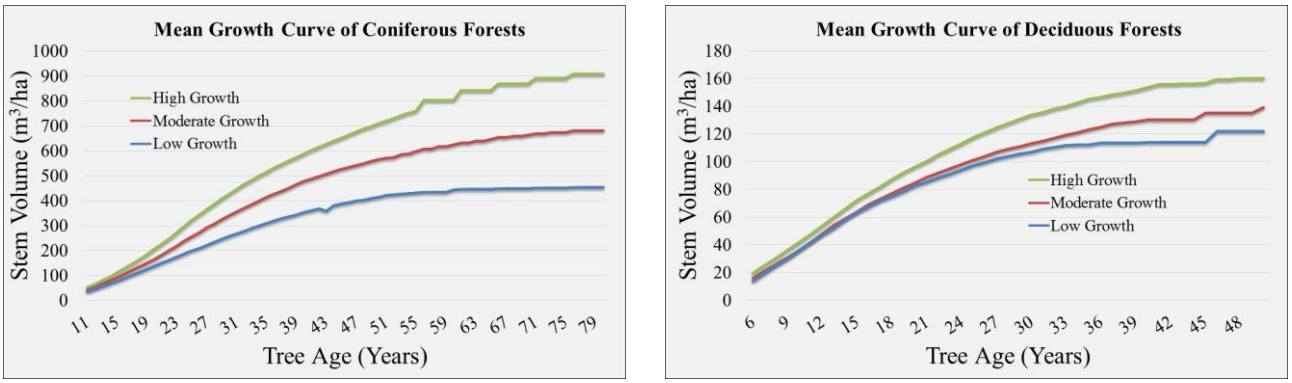

(**a**) (**b**)

Figure 8. Mean growth curve of (**a**) coniferous and (**b**) deciduous broadleaf forests in each growth rate region, computed from the original Oita data.

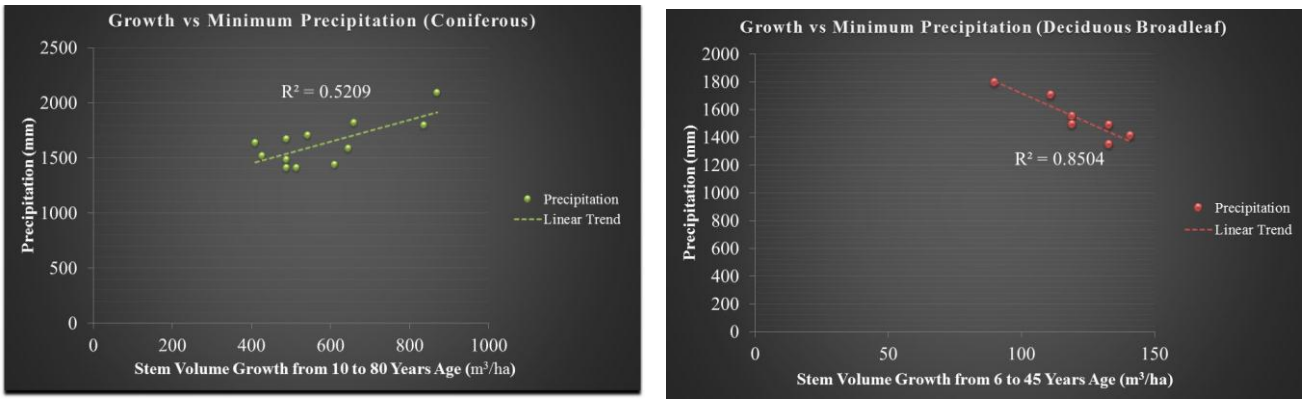

(**a**) (**b**)

Figure 9. Relationship analysis between annual precipitation and tree growth for (**a**) sugi (cedar) trees and (**b**) kunugi (sawtooth oak) trees.

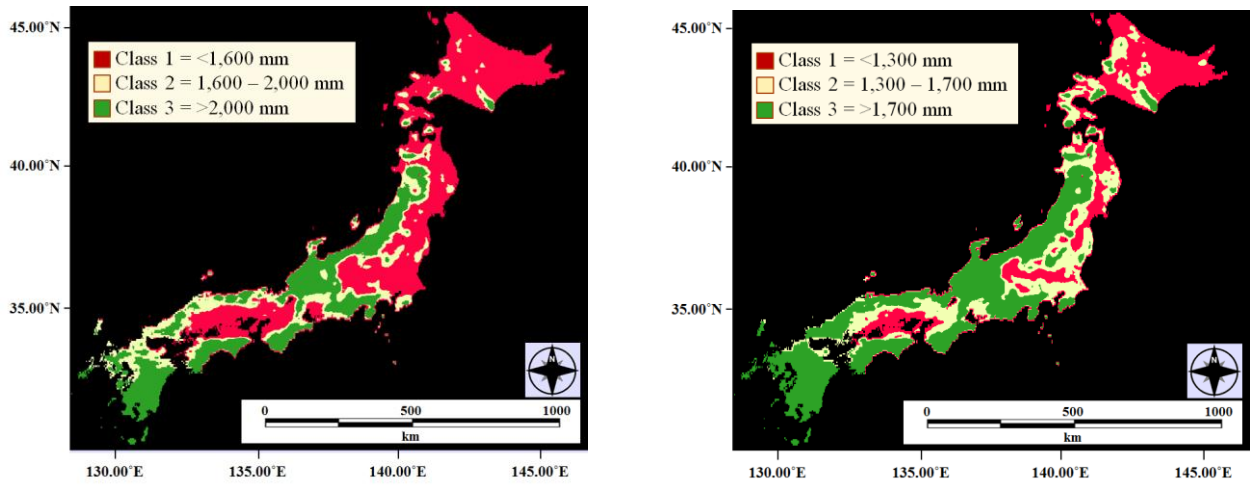

(**a**) (**b**)

Figure 10. Precipitation data classified using the threshold values for evaluating the growth rate of (**a**) coniferous forests and (**b**) deciduous broadleaf forests.

The distribution of the precipitation classes and the thresholds is seen in Figure 10. For the coniferous forests, Class 1 is the area with a low growth rate, Class 2 is moderate, and Class 3 is a high growth rate. For deciduous broadleaf forests, Class 1 is high growth rate, Class 2 moderate, and Class 3 is low growth rate. Finally, Figure 11 shows a graph of the distribution of tree age overlaid with the forest cover data to extract the exact forest types. For the coniferous and deciduous broadleaf forests, the growth rates are considered for the age conversion, however for the evergreen broadleaf it was not, due to the lack of reference data, so that has been converted directly from the stem volume map using the stem volume-age relationship information provided by Sasaki *et al.* [41].

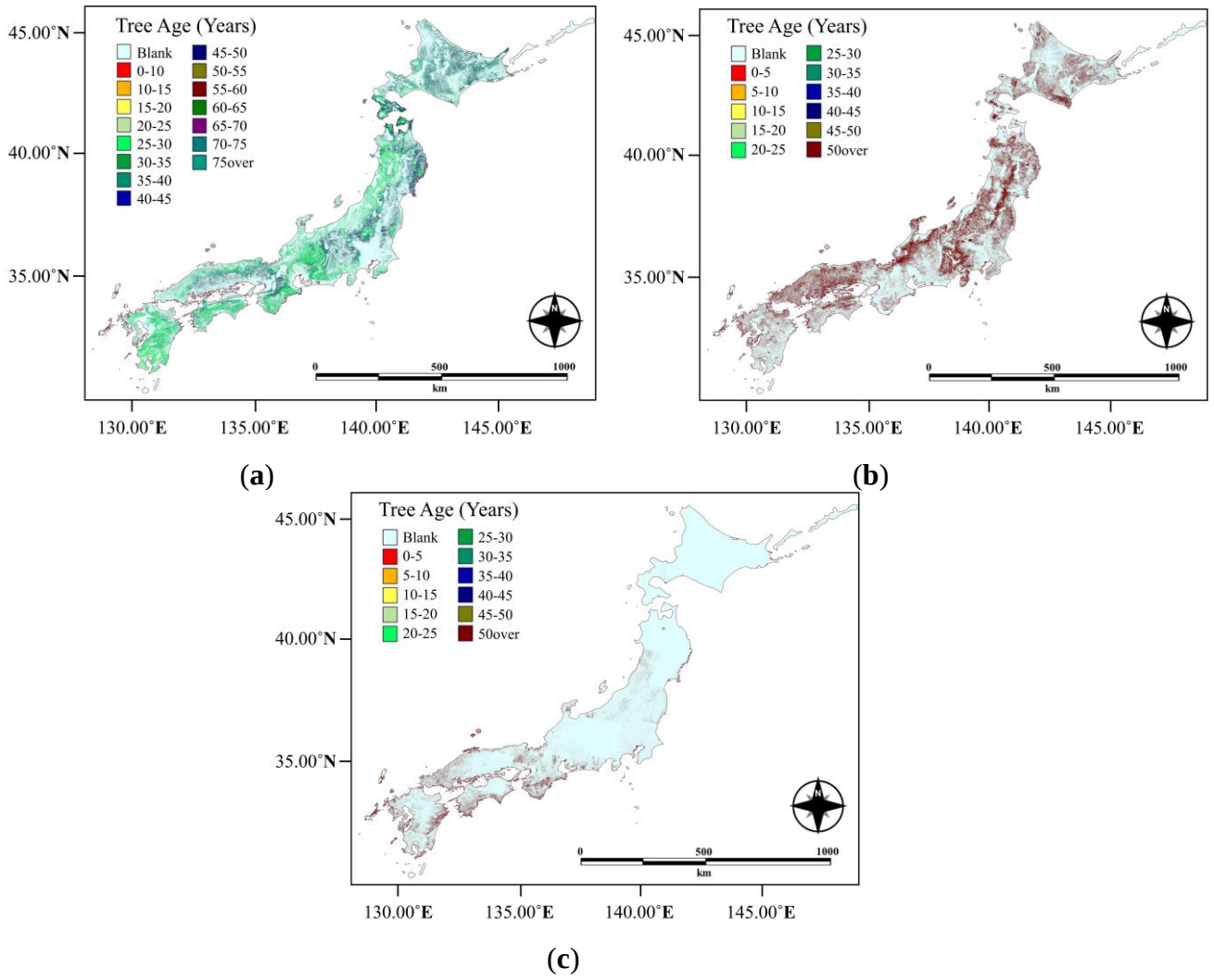

Figure 11. Tree age map transformed from the stem volume map for the (**a**) coniferous, (**b**) deciduous broadleaf and (**c**) evergreen broadleaf forests.

The statistical distribution of forest tree ages can be seen in Figure 12. Coniferous forests can be widely distributed among the different tree ages. The majority lie in the 25–30 year age range for Site 1 (high growth rate regions), 30–35 years range for Site 2 (moderate growth rate regions) and 35–40 years range for Site 3 (low growth rate regions). We can also confirm some sizable areas over 75 years of age, which can be understood to be old mature forested areas left naturally and still growing without any management, while the areas with lower tree ages are places where plantations or forest management is

in operation. However, future work is needed to validate the accuracy of this concept. Compared to coniferous forests, the majority of deciduous and evergreen broadleaf forests can be observed to have tree ages of over 50 years. These forests include few to no areas that are actively managed; they are just left to grow naturally, resulting in a majority of the areas being in highly matured age classes.

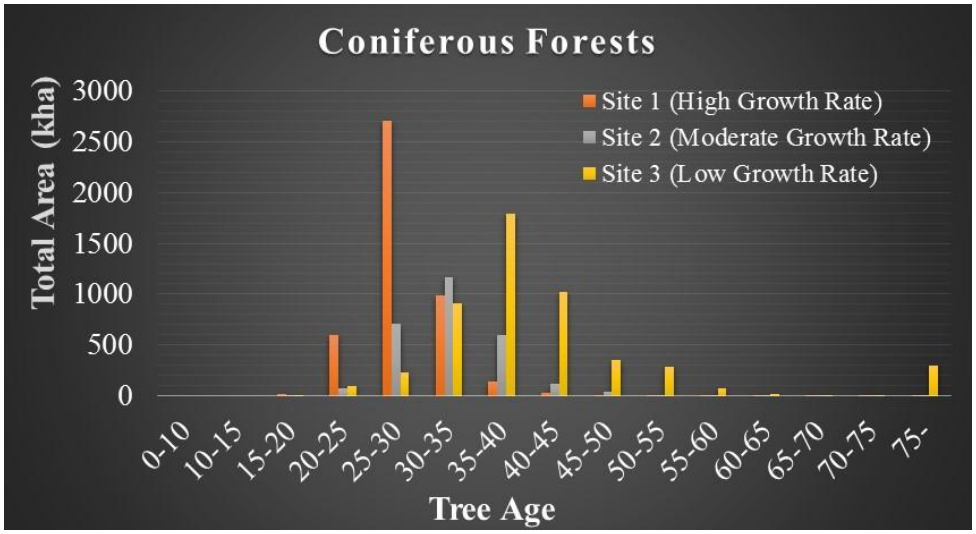

(**a**)

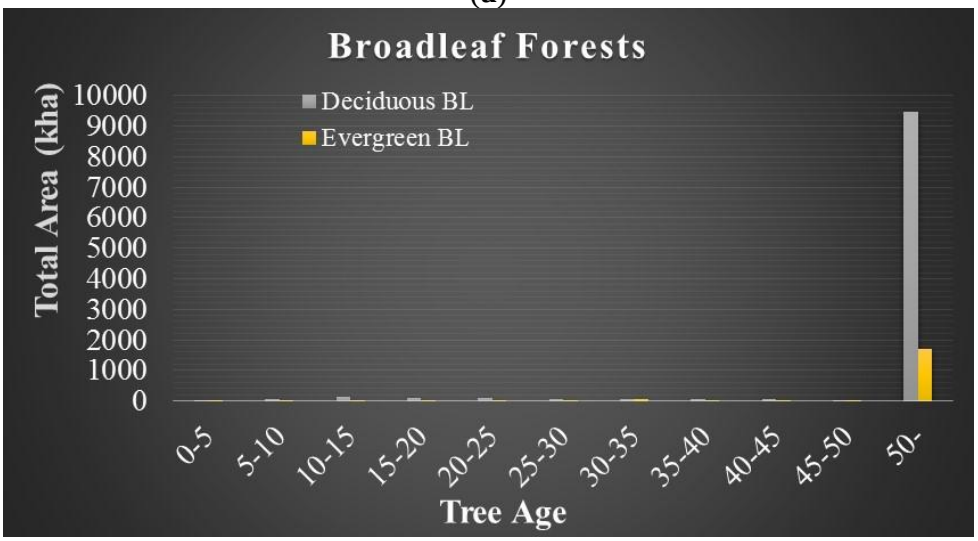

(**b**)

Figure 12. Statistical distribution of forest area by tree age for (**a**) coniferous and (**b**) deciduous/evergreen broadleaf forests in Japan.

4.3.2. CO_2 Sequestration by the Forests of Japan

Estimations of CO_2 sequestration by forest type were obtained by multiplying the observed CO_2 sequestration rates from the Prefectural data by the total area of each forest type's tree age category. Tables 3–5 show the total CO_2 sequestration estimates for coniferous, deciduous broadleaf, and evergreen broadleaf forest age categories, respectively.

Figure 13 shows graphs of the sequestration values among each tree age for (a) coniferous and (b) broadleaf forests. Together with the calculated sequestration value, a mean sequestration value of

each forest type from the reference by Tadaki and Hachiya [15] has been plotted. The coniferous forests show a peak value at approximately 15–20 years of age and then gradually decrease to a value similar to that of the 0–10 year range when they reach 75 years. Each site dependency for the growth rate clearly shows a difference in the total sequestration amount, where compared with trees in low growth rate areas, high growth rate area trees have approximately a 10 t·CO_2/ha/yr difference at the peak value. For the broadleaf forests in this study, the results do not show a large difference between evergreen and deciduous broadleaf forests. The peak value can be observed at approximately 15–20 years of age, which gradually decreases, similar to the coniferous forests; however, the total sequestration value is much smaller than for coniferous forests. It is obvious that Japan has operated a large-scale plantation operation using sugi and hinoki trees because of their fast growth characteristics, which these values reflect. By using the detailed sequestration values for tree ages, sequestration overestimates that implicitly occur with the estimation method using averaged values [15] for coniferous trees of less than 10 years of age and for trees of more than 20 years of age, as well as the underestimation for the peak tree ages (15–20 years), can be avoided altogether. Similarly, for deciduous and evergreen broadleaf forests, compared to the averaged values for all ages, the values for the tree age categories show lower results.

Finally, Figure 14 shows the overall output of the final work, visually illustrating CO_2 sequestration values for forests in Japan.

Table 3. CO_2 sequestration of coniferous forests by tree age using the PALSAR data and the stem volume method.

Forest Type	Age (years)	t·CO_2/ha/yr			Area (ha)			Total Mt·CO_2		
		Site 1	Site 2	Site 3	Site 1	Site 2	Site 3	Site 1	Site 2	Site 3
Coniferous	0–5	3.38	2.56	1.70	0	0	0	0	0	0
	5–10									
	10–15	13.23	9.57	6.20	0	0	0	0	0	0
	15–20	16.11	11.45	6.76	22,826	6,575	7,332	0.37	0.08	0.05
	20–25	12.21	8.49	5.83	592,573	69,564	97,357	7.24	0.59	0.57
	25–30	10.05	7.83	5.34	2,700,597	705,043	230,650	27.15	5.52	1.23
	30–35	8.16	6.74	5.21	989,309	1,168,617	904,797	8.07	7.87	4.72
	35–40	6.42	5.87	4.89	137,687	600,268	1,791,110	0.88	3.52	8.76
	40–45	5.61	5.07	4.41	31,225	122,804	1,023,606	0.18	0.62	4.51
	45–50	5.41	4.63	3.78	7,835	38,352	349,890	0.04	0.18	1.32
	50–55	4.84	4.20	3.30	2,179	5,265	287,697	0.01	0.02	0.95
	55–60	4.08	3.61	2.91	684	7,685	78,352	0.00	0.03	0.23
	60–65	3.35	2.92	2.29	183	877.37	15,174	0.00	0.00	0.03
	65–70	2.47	1.78	1.40	1.57	1,986	9,501	0.00	0.00	0.01
	70–75	2.17	1.41	1.03	0.79	190.96	9,136	0.00	0.00	0.01
	over 75	1.18	0.42	0.42	30.57	1,098	296,715	0.00	0.00	0.13
Total					4,485,131	2,728,325	5,101,317	43.95	18.44	22.52
Overall						12,314,773			85.0	

Table 4. CO_2 sequestration of deciduous broadleaf forests by tree age using the PALSAR data and the stem volume method.

Forest Type	Age (years)	t·CO_2/ha/yr	Area (ha)	Total Mt·CO_2
Deciduous Broadleaf	0–5	2.91	38,756	0.11
	5–10	6.33	58,850	0.37
	10–15	6.50	151,418	0.98
	15–20	6.89	91,892	0.63
	20–25	5.96	90,147	0.54
	25–30	5.20	78,751	0.41
	30–35	5.09	62,852	0.32
	35–40	3.79	48,437	0.18
	40–45	3.52	57,704	0.20
	45–50	3.13	36,219	0.11
	over 50	1.87	9,475,569	17.74
Total			10,190,332	21.61

Table 5. CO_2 sequestration of evergreen broadleaf forests by tree age using the PALSAR data and the stem volume method.

Forest Type	Age (years)	t·CO_2/ha/yr	Area (ha)	Total Mt·CO_2
Evergreen Broadleaf	0–5	2.46	35,540	0.09
	5–10	6.43	33,957	0.22
	10–15	6.57	15,752	0.10
	15–20	6.93	17,987	0.12
	20–25	6.27	20,771	0.13
	25–30	5.32	23,800	0.13
	30–35	5.38	68,927	0.37
	35–40	3.93	31,164	0.12
	40–45	3.74	36,252	0.14
	45–50	3.23	41,367	0.13
	over 50	1.87	1,716,706	3.21
Total			2,042,228	4.76

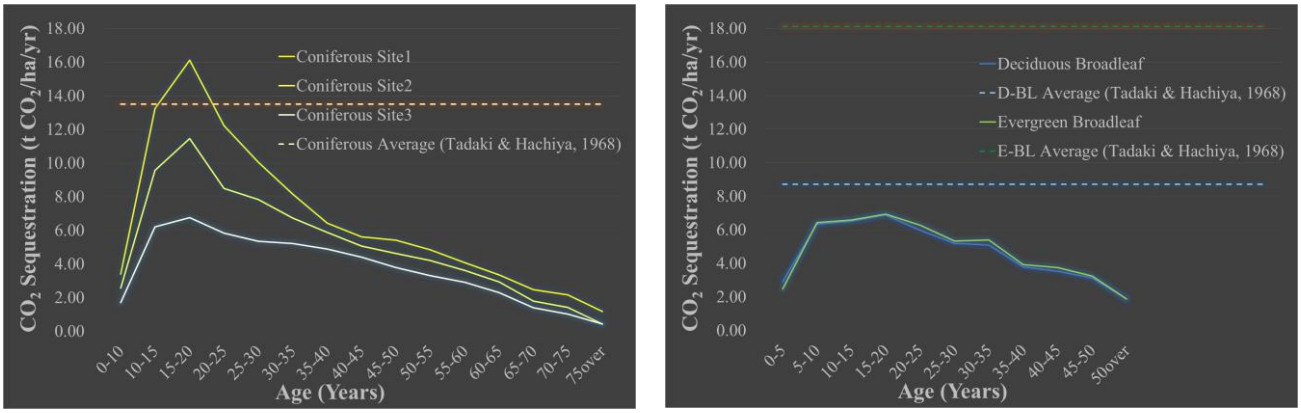

(**a**) (**b**)

Figure 13. Trend of CO_2 values by tree age classes for (**a**) coniferous and (**b**) deciduous/evergreen broadleaf forests.

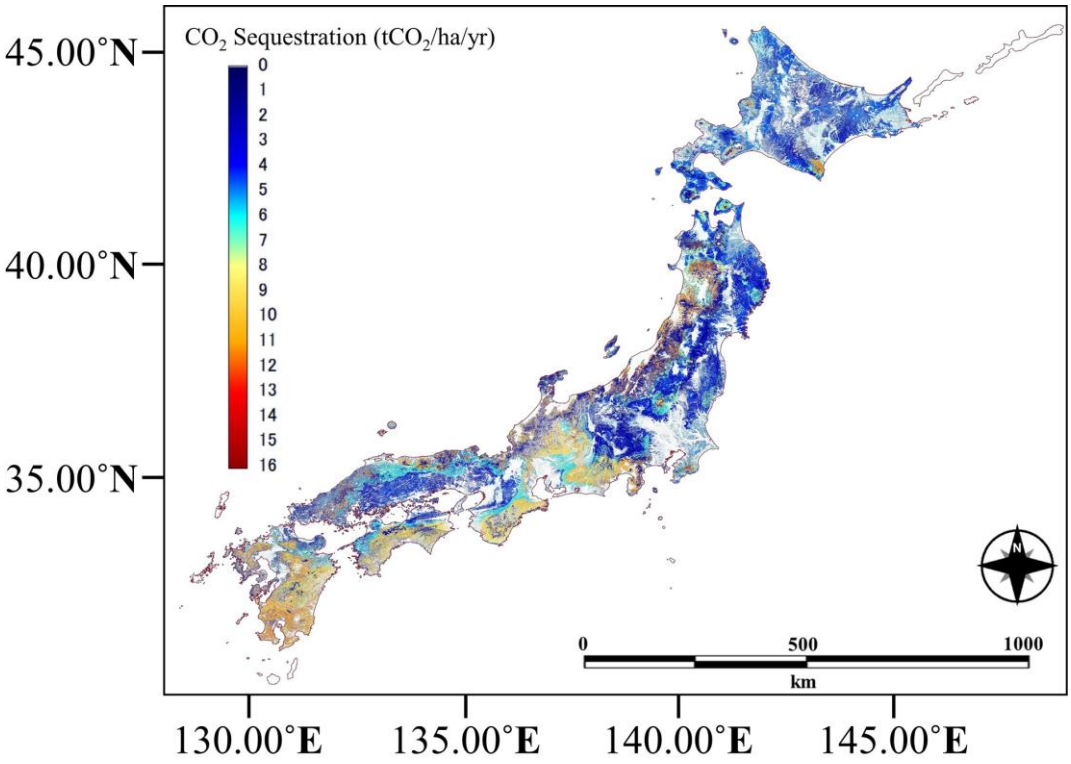

Figure 14. CO_2 sequestration map of Japan.

4.4. CO_2 Sequestration Estimates and Errors

4.4.1. CO_2 Estimates and Potential Errors

The total CO_2 from the forests of Japan has been calculated by taking into consideration both forest type and tree age. It should be understood that determining the accuracy of this result is quite difficult, because there is no known "true value" for this information. It is also necessary to note that there are always sources of error when attempting to calculate such estimations. Possible errors that could generate inaccuracies in the results have been identified and listed here:

1. Accuracy of the land cover map (forest cover map)
2. Dependency on the backscattering model for stem volume estimation
3. Stem volume-age relationship curve
4. The sequestration value itself

Number 1 refers simply to errors resulting from the misclassification of each forest type. As acknowledged in the work, the total area size of a forest type is an important factor in calculating total CO_2 sequestration, because the sequestration value per unit area is multiplied by the total area of each forest type. Figure 15 illustrates the relationship between accuracy and errors for each forest type in reference to the error matrix (Table 2).

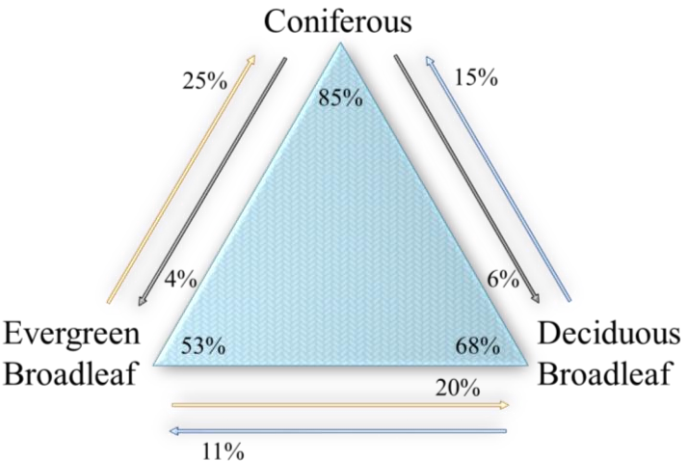

Figure 15. Triangular relationship of the forest classes and their accuracy and errors.

The figure shows the relationship between the classes used in the classification scheme. It indicates the accuracy (percentage value inside the triangle) and errors of omission (outside the triangle). The arrows indicate the misclassification of the classes that might have been classified into one class (beginning of the arrow) but may have instead been classified into a different class (end of the arrow). For example, coniferous forests may have had an 85% accuracy rate in classification, while 4% were misclassified into evergreen broadleaf, and 6% were misclassified into deciduous broadleaf forests. The same can be said for the other two classes. Thus, an 85% accuracy rate for coniferous may be true, but there are 4% and 6% chances of errors due to misclassification into evergreen and deciduous broadleaf forests, respectively, in calculating the total CO_2 amount. The same can be shown for the other classes, mutatis mutandis. The evergreen broadleaf class shows 20% and 25% chances of error from deciduous broadleaf and coniferous forests, respectively, while deciduous broadleaf shows 11% and 15% chances of error from evergreen broadleaf and coniferous forests, respectively.

For number 2, errors in the backscattering model can be explained by the RMSE calculated from the estimated stem volume *versus* the ground truth volume information (Figure 4). As has been explained in an earlier section, the RMSE of the backscattering model resulted in 105.58 m^3/ha. This can lead to errors in transforming the stem volume into the tree age information, and thus become an error in the estimation of CO_2 sequestration. For example, in the coniferous trees in high growth rate areas, a 100 m^3/ha difference can miss the true tree age by ±6 years. Larger differences accrue to lower growth rate areas, for example at Site 3 (low growth rate region) 100 m^3/ha can miss the tree age by ±13 years by looking at the stem volume-age relationship data from the Oita Prefectural Government. A 6-year difference might change the estimation values; for example, the forested coniferous areas at peak ages could be classified to earlier or older age ranges and vice versa: the older age classes could change to the peak tree age classes. Therefore, this error source must be acknowledged as one possible error in the estimation.

For number 3, the tree age transformation used the reference data provided by the Oita Prefectural Government and from Sasaki *et al.* [41]. According to this growth curve, the stem volume information was reclassified for the whole of Japan. The issue here is whether this growth curve also has implications for other regions in Japan. This study used the reference information as a representative growth curve for each tree type, and using the precipitation data, it has been assumed that the other regions of Japan would similarly lie along one of those growth curves. To make sure, additional references were collected

to compare the curve information to other regions of Japan [42,43]. According to the tree growth curve information from the Kagoshima region (Kyushu district) and Aomori region (Tohoku district), there are differences in the growth curves depending on the different site productivity areas; however, comparing the two figures, a large difference between growth curves even in opposite environmental regions (the warmer Kagoshima region, and the cooler Aomori region) cannot be confirmed [42,43]. It is known that there is a most suitable growth curve for each Prefecture in Japan, but this study considered that by making an attempt to normalize the differences of the growth curves by using the precipitation data and setting the threshold. Thus it can be said that the growth curve differences among each region are averaged out and reduced to the least possible error in this aspect. Still, this is one point that could be considered as a potential error in the estimation.

Finally, for number 4, the sequestration information was modified from the Tochigi Prefectural Government by taking the mean or weighted mean of each tree type and using that value as representative of each forest type tree age class. The Prefectural data for the CO_2 sequestration is estimated using the guidelines commonly used for estimations in the forests of Japan, based on the following equation:

$$\begin{aligned}\text{Annual } CO_2 \text{ Sequestration (per ha)} \\ = \text{Annual Growth } (m^3/\text{ha}) \times \text{Biomass Expansion Factor} \\ \times \text{Bulk Density} \times \text{Carbon Content} \times CO_2 \text{ Equivalent Factor}\end{aligned} \quad (6)$$

Annual growth is measured by stem volume growth. The biomass expansion factor is used for expanding the stem volume into an estimate for the whole volume of the tree, including the volume of leaves, branches and roots together. This value usually differs among tree types and species. Bulk Density represents the weight per cubic meter of volume. Carbon content commonly uses the value of 0.5, which means that the wood is composed of approximately 50% carbon. Finally, to convert the carbon value to a CO_2 sequestration value, the CO_2 Equivalent Factor of 44/12 is multiplied, where 12 and 44 are the molecular masses of carbon and CO_2, respectively.

An error that can occur from this is the sequestration value used in multiplying the total forest area, which would be different if it were actually broken down in further detail for each specific tree type and age. Some trees capture more or less CO_2 compared to other tree types within the same forest type, but those values were averaged for this study. Another possible error source is the minimum and maximum sequestration value for each tree age class. Because it is difficult to discriminate between forests using a one-year age distribution, the tree ages were reclassified into 5-year interval ranges. This study used the mean value within that range, and there are minimum and maximum values for those categories, and those can cause errors in the sequestration estimation as well. Table 6 shows the minimum and maximum sequestration values for each forest type at each tree age class range. As shown, there are some classes that have high sequestration values at the peak age of coniferous trees (10–15 years) at site 1, which is both a little higher than the average value from the evergreen broadleaf forests of Tadaki and Hachiya [15] and also similar to the deciduous broadleaf forests. Looking at all the ages, the biggest differences between maximum and minimum can be observed in the peak aged forest classes. This point is one of the more probable errors.

Table 6. CO_2 sequestration minimum and maximum values for each forest type and tree age class.

Coniferous ($t \cdot CO_2/ha/yr$)							Deciduous Broadleaf ($t \cdot CO_2/ha/yr$)			Evergreen Broadleaf ($t \cdot CO_2/ha/yr$)	
	Site 1		Site 2		Site 3						
Age (years)	Min	Max	Min	Max	Min	Max	Age (years)	Min	Max	Min	Max
0–5	3.26	3.49	1.95	2.75	1.23	1.84	0–5	1.72	4.16	1.56	3.44
5–10							5–10	3.80	9.92	3.43	10.29
10–15	11.75	18.43	8.70	11.78	5.38	8.64	10–15	5.06	8.44	5.14	8.57
15–20	14.23	18.08	9.90	13.15	5.99	8.88	15–20	5.17	8.33	5.14	8.57
20–25	11.13	13.23	7.70	9.49	5.29	7.31	20–25	5.08	7.20	5.32	7.60
25–30	9.55	10.93	7.50	8.20	4.68	5.98	25–30	3.97	5.56	4.18	5.70
30–35	7.99	8.71	6.39	6.98	5.03	5.95	30–35	3.60	5.45	3.80	5.70
35–40	6.30	6.71	5.63	6.61	4.55	5.27	35–40	2.12	4.81	2.28	4.94
40–45	5.19	5.91	4.61	5.40	3.85	4.78	40–45	1.86	4.34	1.90	4.56
45–50	4.37	5.89	3.79	5.01	3.46	4.51	45–50	1.86	3.70	1.90	3.80
50–55	3.44	5.75	3.23	4.94	3.02	3.78	50 over	0.60	3.41	1.50	3.61
55–60	2.79	5.82	2.72	4.55	2.58	3.78					
60–65	2.08	5.28	2.01	3.65	1.71	2.93					
65–70	1.32	4.35	1.04	2.77	0.97	1.98					
70–75	1.32	3.89	0.97	2.39	0.97	1.22					
75 over	0.59	2.06	0.22	0.79	0.24	0.53					

4.4.2. Actual CO_2 Estimates Considering the Errors

The CO_2 sequestration amount by the forests in Japan was calculated after each error was taken into consideration as discussed in Section 4.4.1. Table 7 shows the summary of the final output of the total CO_2 amounts when these errors are considered.

In Table 7, the summary of the total CO_2 calculated from this study is listed when each of the error cases is considered. Four different cases of potential errors were examined: land cover misclassification, reliability of the backscattering model, dependency of the tree age curve, and the sequestration value. The tree age curve is listed as N/A because it is simply the errors caused by the growth trend of the trees, and giving an estimation by using other Prefectural Governments' tree age curve information will give results similar to those obtained using the Oita data. However, for the errors from land cover mapping misclassification, backscattering model and sequestration values, and after considering the backscattering model and sequestration value errors together, the estimation was calculated.

In the table, Avg_{val} Min_{val} and Max_{val} represent the average, minimum and maximum sequestration value used for the estimation, respectively. Min_{tot} and Max_{tot} represent the minimum total and maximum total CO_2 sequestration by each category, respectively. Thus, for backscattering model error cases in the coniferous category, the total CO_2 amount was estimated using the average sequestration value (the value listed in Table 3). Values in brackets written after N/A are the total sequestration outputs listed in the tables of deciduous and evergreen broadleaf forests (Tables 4 and 5).

Table 7. Summary of total CO_2 sequestration estimated after considering each possible error source.

Error Types / Forest Types	Coniferous		Deciduous Broadleaf		Evergreen Broadleaf		Total CO_2 Sequestration	
	Unit: Mt·CO_2							
Land Cover Mapping	Min_{tot}: 50.94	Max_{tot}: 89.67	Min_{tot}: 20.29	Max_{tot}: 25.50	Min_{tot}: 4.57	Max_{tot}: 11.94	Min_{tot}: 75.80	Max_{tot}: 127.11
Backscattering Model	(Avg_{val}) Min_{tot}: 65.46	(Avg_{val}) Max_{tot}: 99.81	N/A (21.61)		N/A (4.76)		Min_{tot}: 91.83	Max_{tot}: 126.18
Tree Age Curve	N/A		N/A		N/A		N/A	
Sequestration Value	Min_{tot}: 78.80	Max_{tot}: 90.97	Min_{tot}: 7.38	Max_{tot}: 31.94	Min_{tot}: 6.55	Max_{tot}: 14.78	Min_{tot}: 92.73	Max_{tot}: 137.69
Backscattering Model + Sequestration Value	(Min_{val}) Min_{tot}: 64.65 (Max_{val}) Min_{tot}: 75.03	(Min_{val}) Max_{tot}: 91.45 (Max_{val}) Max_{tot}: 110.64	N/A (21.61)		N/A (4.76)		(Min_{val}) Min_{tot}: 91.02 (Max_{val}) Min_{tot}: 101.4	(Min_{val}) Max_{tot}: 117.82 (Max_{val}) Max_{tot}: 137.01

Errors of misclassification were considered by using the percentage of the total area of each distributed forest class modified based on the actual misclassification percentage shown in Figure 15. For example, 4% and 6% of coniferous classes were misclassified to evergreen broadleaf and deciduous broadleaf forests, respectively. Thus, 4% and 6% of the total area from those forest classes, respectively, were subtracted and added to the coniferous class (this is determined as the maximum status). At that point, the deciduous and evergreen broadleaf status was determined as the minimum status. On the other hand, 25% and 15% were misclassified to the coniferous class when they were likely to be evergreen and deciduous broadleaf forests, respectively. Similarly, those percentages of the total area were subtracted from the coniferous forests and added to the evergreen and deciduous broadleaf forest classes (this is determined as the minimum status). Again, at this point, the maximum deciduous and evergreen broadleaf statuses were determined. The dependency of the classification results to errors in estimates of sequestration were assumed in this method. As a result, the minimum total sequestration was 75.80 Mt·CO_2, while the maximum was 127.11 Mt·CO_2. Here, the sequestration value by tree age class for each forest type does not change, and only the total area of the forests fluctuates. We can see how the total size of the forested area is one important factor that contributes to total sequestration.

Errors of the backscattering model were considered from the developed RMSE model, which resulted in 105.58 m^3/ha. According to the stem volume-tree age curve information, the difference of stem volume results in 6-year, 7-year and 10-year differences for the coniferous trees on site 1, site 2 and site 3, respectively. Using this information, the estimation of the CO_2 in coniferous forests was re-assessed by shifting the age range by the above tree age year difference. The minimum and maximum then became 65.46 and 99.81 Mt·CO_2, respectively. The total CO_2 was then calculated using these values along with the total values of other forest types (deciduous broadleaf (DBL) and evergreen broadleaf (EBL)). The

estimation was made only for the coniferous forests in this case because the actual error values of the model developed by Wijaya [38] were not found.

For the sequestration value errors listed in Table 6, the minimum and maximum values were applied, multiplying by the total forested area of each forest type. Overall total CO_2 resulted in 92.73 $Mt{\cdot}CO_2$ and 137.69 $Mt{\cdot}CO_2$ for minimum and maximum totals, respectively. This case is easier to interpret compared to the other errors because all the forest classes can be estimated clearly.

Finally both the errors from the backscattering model and the sequestration value were added, and then the estimation was re-assessed. This was conducted only for the coniferous class, and resulted in 64.65 $Mt{\cdot}CO_2$ and 91.45 $Mt{\cdot}CO_2$ for minimum and maximum amounts, respectively, when the minimum sequestration value (Table 6) was used, and 75.03 $Mt{\cdot}CO_2$ and 110.64 $Mt{\cdot}CO_2$ for minimum and maximum amounts, respectively, when the maximum sequestration value (Table 6) was used.

5. Discussion

5.1. Stem Volume Empirical Modeling

In Section 4.1, an empirical backscattering model was developed to estimate stem volume information across the forests of Japan. The challenge is that backscattering can have multiple causes within a forested area, and can be affected by species, structures, soil moisture [44], density of forests [18], *etc.* A simple empirical modeling method was used by taking a correlation analysis between the backscattering intensity and the ground reference data. We have avoided most of the possible distracting factors affecting the difference in the backscattering to make a more accurate trend between the parameters and SAR image, which allowed a better interpretation when compared to many studies performed in similarly rugged areas [24]. We could discuss about the limitation of L-band SAR for the estimation of biomass, due to its sensitivity which gives saturation at a certain biomass level [45], however the most important variable in our study is the topographic effect. Although various radiometric corrections have been developed to normalize the SAR imagery [19,26,27,46] the radiometric accuracies of those correction methods can always be challenged. However, without their application, the topographic effects caused by rugged terrain will remain a crucial issue, especially for the study area here in Japan, and can result in higher errors compared to not applying them. There might be solutions to improve the interpretation of the modeling, but in this first study on national-scale estimation using remote sensing, we believe that the result can serve as a standard. Note that during the relationship analysis, speckle filtering was not applied to the PGM data. This decision was made because the data were downscaled to 25 m resolution from the original, which averaged out the area, reducing the noise. Further filtering might lose the actual information from the surface objects. However, in the future, a different filtering method might be applied to evaluate whether the difference affects the results.

5.2. Land Cover Mapping of Japan

A land cover map was produced that not only defined the areas as simple forests and non-forested areas but also provided more detail (*i.e.*, subclasses) such as forest types (coniferous, deciduous and evergreen broadleaf), so the information could be used in many different ways. The need for a detailed digital land cover (or digital vegetation model) map, especially for the vegetation categories, is important

for obtaining more precise estimations of CO_2 sequestration values. For this study, only single-scene data sets were used to develop the land cover map for each area. Sanga-Ngoie *et al.* [5] states the usefulness of applying temporal data sets to improve land cover accuracy due to the clear difference of radiance values that change during different seasons of the year. In the case of forest classes, similar spectral signatures would be observed throughout a season after blooming finishes, but clear and distinguishable differences can be observed for different forest types, such as trees whose leaves fall in the winter. Such methods were not applied in this case because few cloud-free products were captured, which made it difficult to find a set of scenes with two different seasons for each location. Operation of Landsat 8 is still in its third year, so its scene database is still relatively small compared to Landsat 5 or 7, so such methods are currently limited to very small areas or must wait for more data to be collected over time.

However, because of the lack of temporal data scenes, the classification process was performed not by increasing the number of images but by collecting as many detailed training sites as possible. This method led to the ability to discriminate between forest classes in more detail and with more precision, because constructing more detailed and precise land cover classes resulted in greater chances of unclear pixels being classified into the forest class to which they should correctly belong. For example, if the training sites of the forest classes are specified and classified only as "coniferous, deciduous broadleaf and evergreen broadleaf", deciduous and evergreen broadleaf forest classification drop inaccuracy by 33% and 36%, respectively, compared to when more detailed training classes of those forest types are constructed. Therefore, this methodology is effective when there are few scenes available for classifying a region. Constructing detailed training sites can improve the categorical map. In the future, we recommend reprocessing the classification of areas that had lower accuracy results or regions that were covered by snow/cloud to improve and correct the land cover types used here.

5.3. Stem Volume Method for CO_2 Sequestration Estimates

5.3.1. CO_2 Sequestration Values and Trends

The conventional method [15], when used alone for estimating CO_2 sequestration, results in large errors in the total amount compared to methods that give special attention to tree age. The stem volume method for discriminating tree ages within each forest type clearly shows the importance of this variable for avoiding over- or underestimations, depending on the growth stage of the forests examined. The use of L-band SAR data rather than optical data [5] made this discrimination possible, yielding sequestration rates by tree age for trees up to 75 years of age for coniferous and 50 years of age for deciduous and evergreen broadleaf forests. It is thus clearly established that sequestration rates of 13.5 t·CO_2/ha/yr [15] are only valid for 10–15-year-old coniferous forests in high growth rate regions. In contrast, deciduous broadleaf forests reach just below the 8.7-t·CO2/ha/yr threshold only in the 15–20-year-old range. For evergreen broadleaf forests, this is a large issue when the conventional method is applied, because it shows approximately 3 times greater value than observed in the results of this study, meaning that there would be a large overestimation of the forest carbon sink capacity if such a value is applied. High sequestration values from evergreen broadleaf forests are difficult to confirm for many reasons; however, the amount of sequestration by evergreen trees in Japan is acknowledged to depend on total solar

radiation and air temperature. Gross Primary Product (GPP) results from the total radiation, while the Net Primary Product (NPP) is set by the amount of respiration subtracted from the GPP [47]. In this case, higher air temperature leads to higher respiration and decreases the NPP. On the other hand, when both total radiation and air temperature are low, respiration rates decrease but NPP becomes the same or even greater compared to higher radiation periods [37]. Depending on the season and location of the observation, the average value of evergreen broadleaf forests will differ, and it might well be possible that the large value obtained by Tadaki and Hachiya [15] resulted from such causes.

It is very important to note that the averaged sequestration value for the coniferous forest type matches the sequestration value by tree ages obtained here for the 10–15-year-old coniferous trees at Site 1. This is also the category of the second fastest-growing period for coniferous trees at that site. The same is also true for deciduous broadleaf forests for 15–20-year-old trees; it is just a little lower than the average value. This strongly implies that an estimation based on the averaged values alone will round up the values for trees in different growth stages, causing an overall overestimation of the carbon sink capacity [5], both for natural and planted forests. The results emphasize the fact that sequestration differs among tree ages. This reality should be taken into consideration in all cases, otherwise, erroneous values of the forests sequestration capacity will be obtained, generating results that possibly have errors from using less accurate values.

The uncertainty assessment gave a clear view of how and why the estimations can fluctuate, where the estimated total CO_2 lies between the minimum 75.80 Mt·CO_2 and maximum 137.69 Mt·CO_2. The minimum estimate results from land cover error and the maximum from sequestration value error. After examining the results presented in this paper, it can be assumed that these two parameters are the most important factors when estimating sequestration amounts. Focusing on the results where 111.27 Mt·CO_2 was shown, the fluctuation of the estimated amount is a difference of approximately 23 to 32%. Certainly, if the errors for the DBL and EBL classes for the backscattering model errors could be obtained, some change might be observed in the results; however, it may be determined that even if this occurred, it would not result in a very large difference from the current numbers. Through the uncertainty assessment, a better understanding of the fluctuation of the CO_2 trend became clear, and thus this result leads to a strong confidence in the practical usage of this methodology.

5.3.2. Validity of the Method in Comparison

For further knowledge, other estimation methods were investigated and compared to the results of this study. Four main methods were examined and compared; one is from this study, the second is from the conventional method by Tadaki and Hachiya [15], the third is the work conducted by Sasaki and Kim [7], and the last is from the National Institute for Environmental Studies (NIES) [8] of the IPCC report for the forest carbon sink. The total CO_2 estimation is summarized in Table 8 [7,8,15] for all four methods. For the conventional method, the sequestration value was used along with the total forest areas obtained from our work.

Table 8. Summary of the total CO_2 sequestration estimated by various methodologies in the different studies.

Methods	Total CO_2 Sequestration
Conventional (Tadaki and Hachiya [15])	308.51 Mt·CO_2
Sasaki and Kim [7]	73.7 Mt·CO_2
NIES [8]	77.67 Mt·CO_2
Stem Volume Method (our work)	111.27 Mt·CO_2

The stem volume method used in this study, shows a result of 111.27 Mt·CO_2 by considering both forest type and tree age information (coniferous: 85.0 Mt·CO_2; deciduous broadleaf: 21.61 Mt·CO_2; evergreen broadleaf: 4.76 Mt·CO_2). With the conventional method [15] using the averaged value compared to the results in this study, a large overestimation of the sequestration can be observed, because the sequestration value dumps everything into one category, omitting tree age information and ignoring lower sequestration stages, leading to high overestimation of the result. Sasaki and Kim [7] and NIES [8] show similar estimation values, however for the former study, the result is obtained by using the land use model and carbon stock growth model and estimates the sequestration value classifying the forests as planted and natural forests. Planted forests showed an estimation of 56.1 Mt·CO_2, while natural forests were estimated at 17.6 Mt·CO_2, and then summed for a total result of 73.7 Mt·CO_2. The most interesting result is from the NIES, whose approach used forest registration data from each prefectural government and differentiated the forests by tree type, collecting annual growth information for each, and then performing an estimation by multiplying the annual sequestration value by the total forested area of each tree type, which is similar to this work. They have not only made calculations for aboveground sequestration but also for the litter and soil. However, the majority of the sequestration results from the aboveground biomass (aboveground: 76.53 Mt·CO_2; litter: 0.41 Mt·CO_2; soil: 2.58 Mt·CO_2; dead tree: −1.85 Mt·CO_2). If we assume that the methods used by the NIES [8] study are likely to be the most accurate estimation of the natural environment, the remote sensing method applied in this study shows only a 43% overestimation in comparison. This difference can be explained from the errors discussed in the previous section. If methods are developed to reduce those potential errors, our results may become somewhat similar to the results by the NIES. However, even though the NIES results raise some questions, such as the uncertainty of the total forest area, which is important as mentioned, total CO_2 is calculated by multiplying the sequestration value by the total forested areas. The data from prefectural government is sometimes unclear, especially in terms of the area that the forest covers, as researchers have noted (the uncertainty rate of NIES estimates shows 5% for forest areas without discriminating by forest type [8]), so there is a possibility that the NIES is underestimating forest capacity. What is significant about this work compared to the NIES is that this method can be performed throughout various seasons in the future in less time and with lower labor costs through the use of remote sensing data. The work performed by NIES is possible in countries where a large database of forest information is compiled for use in applications, but in countries where this is not the case, it will be very difficult to implement such a method. On the other hand, the method developed in this study can be applied in any country as long as the required data sets are available. Moreover, the uncertainty of the total forest area compared to NIES can be overcome using our methodology, because the correct amounts and locations of forests are easier to discern. Overall, this study explains why the result is much lower (better) than the

conventional method, which seems to result in high overestimation, while when compared to NIES results, the estimation arrived at by this study does not show serious underestimation. The true result likely falls between the two as discussed in this paper. The results achieved using the stem volume method in this study show both an improvement and the potential for obtaining even better results than other methods by using remote sensing method. As a note, the term sequestration used in this study can be described as NPP, while the NIES result can be described as Net Ecosystem Product (NEP) because it also considers decomposers. In the future, improvements in the methodology will likely take this into consideration and obtain NEP values of the forests so we can estimate a more precise value not only for use in forest management and policy but also for use in modeling the biogeochemical cycle of terrestrial ecosystems.

6. Concluding Remarks

Rapid change in climatic conditions in recent years has raised many pressing issues and problems that need to be solved. These are of global interest among researchers, companies, politicians and others. Therefore, in response, various measures are being taken, such as the Kyoto Protocol, REDD+ and others, to mitigate the impacts of climate change. Although such policies and actions are being implemented around the world, the quantitative estimation of how well they have contributed to the natural environment, such as in terms of carbon sequestration, is still under discussion. Meanwhile, this work has shown a path forward in quantitative estimates on a national scale for CO_2 sequestration by utilizing fine resolution satellite imagery through a local/regional scale analysis. Focusing on forest type and tree age information using the LANDSAT and PALSAR data, respectively, yields more accurate data. This methodology gives better interpretations and more precise estimations of CO_2 sequestration, as it is clear that without both tree type and tree age discrimination, overestimations may well result.

The CO_2 amount and other important information revealed in this study has provided important data. Do old mature trees sequestrate as much as younger trees? The answer is no when we see the trend of the sequestration as a function of tree age. Using this information, we can discuss policies such as the REDD+ procedure. Is planting trees for 100 years' time [48] for a credit really an effective and correct way to manage forest resources? Rather, it could be suggested that planting faster growing trees in a period of 20 to 30 years and then replacing them continuously might be more sustainable and effective, even in economic terms. The findings in this paper can thus suggest these types of ideas to policy makers for more sustainable development/conservation.

The methodology is not only of interest for forestry, stakeholders, and policy makers but also for researchers who address modeling of the earth's ecosystems. The knowledge of CO_2 trends in the terrestrial biosphere developed from this work contributes to a better understanding of the biogeochemical cycle and thus sheds more light on the influence of the terrestrial ecosystem and its interaction with the atmosphere. This could lead to a step forward in understanding more about climatic systems. Utilizing fine resolution satellite imagery on a more local/regional scale can be expected to improve modeling accuracy and help better understand the trends of the earth's systems.

The in-depth quantification of forest sequestration can play an important role in many fields, helping them to improve how they set strategic actions into operation. Promoting such methods will certainly

support further development and discussion to make a difference in solving or mitigating the issues faced in a more effective way.

Acknowledgments

The authors would like to give their heartfelt appreciation to Kazadi Sanga-Ngoie for cooperating to strengthen the methodology of this study. The authors would also like to thank the Oita Prefectural Government, Forest Management Division Department of Agriculture Affairs along with the Chiba Prefectural Government for providing the forest inventory data.

Author Contributions

K.I. and R.T. conceived this research. K.I. collected the data, performed and analyzed the experiments and drafted the manuscript. R.T. supervised throughout the research and edited the manuscript.

Conflicts of Interest

The authors declare no conflict of interest.

References

1. Hewitt, C.N.; Jackson, A. *Handbook of Atmospheric Science: Principles and Applications*; Blackwell: Padstow, UK, 2003.
2. Chiras, D.D. *Environmental Science*, 7th ed.; Jones and Bartlett: Massachusetts, UK, 2006.
3. Ministry of Agriculture, Forestry and Fisheries (MAFF) of Japan (2010). Annual Report on Forest and Forestry in Japan (Summary). Available online: http://www.rinya.maff.go.jp/j/kikaku/hakusyo/22hakusho/pdf/22_e.pdf (accessed on 6 August 2015).
4. Ministry of Economy, Trade and Industry (METI) of Japan (2005). Kyoto Protocol Target Achievement Plan. Available online: http://www.meti.go.jp/policy/energy_environment/global_warming/study_policy.html (accessed on 6 August 2015). (In Japanese)
5. Sanga-Ngoie, K.; Iizuka, K.; Kobayashi, S. Estimating CO_2 sequestration by forests in Oita Prefecture, Japan, by combining Landsat ETM+ and ALOS satellite remote sensing data. *Remote Sens.* **2012**, *4*, 3544–3570.
6. Hiroshima, T.; Nakajima, T. Estimation of sequestered carbon in article-3.4 private planted forests in the first commitment period in Japan. *J. For. Res.* **2006**, *11*, 427–437.
7. Sasaki, N.; Kim, S. Biomass carbon sinks in Japanese forests: 1966–2012. *Forestry* **2009**, *82*, 113–123.
8. National Institute for Environmental Studies Japan (NIES), Center for Global Environmental Research (CGER). National Greenhouse Gas Inventory Report of Japan. Available online: http://www.gio.nies.go.jp/aboutghg/nir/2014/NIR-JPN-2014-v3.0.pdf (accessed on 6 August 2015).
9. Gibbs, J.K.; Brown, S.; Niles, J.O.; Foley, J.A. Monitoring and estimating tropical forest carbon stocks: Making REDD a reality. *Environ. Res. Lett.* **2007**, *2*, 1–13.
10. Goetz, S.J.; Prince, S.D.; Goward, S. N; Thawley, M.M.; Small, J. Satellite remote sensing of primary production: An improved production efficiency modeling approach. *Ecol. Model*. **1999**, *122*, 239–255.

11. Pachavo, G.; Murwira, A. Remote sensing net primary productivity (NPP) estimation with the aid of GIS modelled shortwave radiation (SWR) in a southern African Savanna. *Int. J. Appl. Earth Obs. Geoinf.* **2014**, *30*, 217–226.
12. Zheng, G.; Chen, J.J.; Tian, Q.J.; Ju, W.M.; Xia, X.Q. Combining remote sensing imagery and forest age inventory for biomass mapping. *J. Environ. Manag.* **2007**, *85*, 616–623.
13. Turner. D.P.; Ritts, W.D.; Cohen, W.B.; Gower, S.T.; Running, S.W.; Zhao, M.; Costa, M.H.; Kirschbaum, A.A.; Ham, J.M.; Saleska, S.R.; *et al*. Evaluation of MODIS NPP and GPP products across multiple biomes. *Remote Sens. Environ.* **2006**, *102*, 282–292.
14. Turner, D.P.; Guzy, M.; Lefsky, M.A.; Ritts, W.D.; Tuyl, S.V.; Law, B.E. Monitoring forest carbon sequestration with remote sensing and carbon cycle modeling. *Environ. Manage.* **2004**, *33*, 457–466.
15. Tadaki, Y.; Hachiya, K. *Forest Ecosystems and Their Productivity*; Ringyo Kagakugijutsu Shinkosho: Tokyo, Japan, 1968. (In Japanese)
16. Ministry of Agriculture, Forestry and Fisheries (MAFF) of Japan (2010). Function of the Sequestration of Forests/Trees. Available online: http://www.rinya.maff.go.jp/kinki/hyogo/mori-grow/mori-co2.html (accessed on 6 August 2015). (In Japanese)
17. Ministry of Environment (MOE) of Japan. Vegetation Distribution of Japan. Available online: http://www.vegetation.biodic.go.jp/zu/index.html (accessed on 9 September 2015). (In Japanese)
18. Iizuka, K.; Tateishi, R. Simple relationship analysis between L-band backscattering intensity and the stand characteristics of sugi (*Cryptomeria japonica*) and hinoki (*Chamaecyparis obtusa*) trees. *Adv. Remote Sens.* **2014**, *3*, 219–234.
19. Castel, T.; Beaudoin, A.; Stach, N.; Stussi, N.; Le Toan, T.; Durand, P. Sensitivity of space-borne SAR data to forest parameters over sloping terrain. Theory and experiment. *Int. J. Remote Sens.* **2001**, *22*, 2351–2376.
20. Dobson, M.C.; Ulaby, F.T.; Le Toan, T.; Beaudoin, A.; Kasischke, E.S.; Christensen, N. Dependence of radar backscatter on coniferous forest biomass. *IEEE Trans. Geosci. Remote Sens.* **1992**, *30*, 412–415.
21. Harrell, P.; Kasischke, E.S.; Bourgeau-Chavez, L.L.; Haney, E.; Christensen, N.L. Evaluation of approaches to estimating aboveground biomass in southern pine forests using SIR-C data. *Remote Sens. Environ.* **1997**, *59*, 223–233.
22. Saatchi, S.S.; Moghaddam, M. Estimation of crown and stem water content and biomass of boreal forest using polarimetric SAR imagery. *IEEE Trans. Geosci. Remote Sens.* **2000**, *38*, 697–709.
23. Sandberg, G.; Ulander, L.M.H.; Fransson, J.E.S.; Holmgren, J.; Le Toan, T. L- and P-Band backscatter intensity for biomass retrieval in hemiboreal forest. *Remote Sens. Environ.* **2011**, *115*, 2874–2886.

24. Chen, E.; Li, Z.Y.; Ling, F.L.; Lu, Y.; He, Q.S.; Fan, F.Y. Forest volume density estimation capability of ALOS PALSAR data over hilly region. In Proceedings of 4th International Workshop on Science and Applications of SAR Polarimetry and Polarimetric Interferometry (PolInSAR), Frascati, Italy, 26–30 January 2009.
25. Small, D. Flattening gamma: Radiometric terrain correction for SAR imagery. *IEEE Trans. Geosci. Remote Sens.* **2011**, *49*, 3081–3093.
26. Japan Aerospace Exploration Agency (JAXA). PALSAR Calibration Factor Updated. Available online: http://www.eorc.jaxa.jp/en/about/distribution/info/alos/20090109en_3.html (accessed on 6 August 2015).
27. Shimada, M. Ortho-Rectification and slope correction of SAR data using DEM and its accuracy evaluation. *IEEE J. Sel. Topics Appl. Earth Obs*. **2010**, *3*, 657–671.
28. Iizuka, K.; Tateishi, R. Analysis of backscattering characteristics of L-band SAR over the mountainous region of Chiba Japan, using 50 m PALSAR mosaic product. In Proceedings of International Symposium on Remote Sensing, Chiba, Japan, 22–26 April 2013.
29. Japan Aerospace and Exploration Agency (JAXA). PALSAR 50 m Orthorectified Mosaic Product. Available online: http://www.eorc.jaxa.jp/ALOS/en/kc_mosaic/kc_mosaic.htm (accessed on 6 August 2015).
30. Cartus, O.; Santoro, M.; Kellndorfer, J. Mapping forest aboveground biomass in the northeastern United States with ALOS PALSAR dual-polarization L-band. *Remote Sens. Environ.* **2012**, *124*, 466–478.
31. Santoro, M.; Beer, C.; Cartus, O.; Schmullius, C.; Shvidenko, A.; McCallum, I.; Wegmüller, U.; Wiesmann, A. Retrieval of growing stock volume in boreal forest using hyper-temporal series of Envisat ASAR ScanSAR backscatter measurements. *Remote Sens. Environ.* **2011**, *115*, 490–507.
32. Zhou, Z.-S.; Lehmann, E.; Wu, X.; Caccetta, P.; McNeill, S.; Mitchell, A.; Milne, A.; Tapley, I.; Lowell, K. Terrain slope correction and precise registration of SAR data for forest mapping and monitoring. In Proceedings of International Symposium for Remote Sensing of the Environment, Sydney, NSW, Australia, 10–15 April 2011.
33. Kobayashi S.; Sanga-Ngoie, K. The integrated radiometric correction of optical remote sensing imageries. *Int. J. Remote Sens.* **2008**, *29*, 5957–5985.
34. Li, W.; Du, Z.; Ling, F.; Zhou, D.; Wang, H.; Gui, Y.; Sun, B.; Zhang, X. A comparison of land surface water mapping using the Normalized Difference Water Index from TM, ETM+ and ALI. *Remote Sens.* **2013**, *5*, 5530–5549.
35. Motohka, T.; Nasahara, K.N.; Oguma, H.; Tsuchida, S. Applicability of green-red vegetation index for remote sensing of vegetation phenology. *Remote Sens.* **2010**, *2*, 2369–2387.
36. Congalton, R.G.; Green, K. *Assessing The Accuracy of Remotely Sensed Data: Principles and Practices*, 2nd ed.; CRC/Taylor & Francis: New York, NY, USA, 2009.
37. Perry, D.A.; Oren, R.; Hart, S.C. *Forest Ecosystems*, 2nd ed.; The Johns Hopkins University Press: Baltimore, MD, USA, 2008.
38. Wijaya, A. Evaluation of ALOS-PALSAR mosaic data for estimating stem volume and biomass: A case study from tropical rainforest of central Indonesia. *J. Geogr.* **2009**, *2*, 14–21.
39. Ministry of Environment (MOE) of Japan. National Survey on the Natural Environment. Available online: http://www.biodic.go.jp/english/J-IBIS.html (accessed on 6 August 2015).

40. Congalton, R.G.; Mead, R.A. A quantitative method to test for consistency and correctness in photointerpretation. *Photogramm. Eng. Remote Sens.* **1983**, *49*, 69–74.
41. Sasaki, H.; Hayashi, H.; Ise, S. Considerations on the selective logging updating of evergreen broadleaf forests. *Tokushima Prefect. For. Res. Cent. Rep.* **1989**, *27*, 22–29. (In Japanese)
42. Forestry Agency. Aomori Region Sugi Tree Rinbun-Shukaku-Hyou (1962). Available online: http://www.ffpri.affrc.go.jp/labs/shukakushiken/02gyoken/02gyoken_28.pdf (accessed on 6 August 2015). (In Japanese)
43. Forestry Agency. Kagoshima Region Sugi Tree Rinbun-Shukaku-Hyou (1965). Available online: http://www.ffpri.affrc.go.jp/labs/shukakushiken/02gyoken/02gyoken_33.pdf (accessed on 6 August 2015). (In Japanese)
44. Ulaby, F.T.; Sarabandi, K.; McDonald, K.; Whitt, M.; Dobson, C. Michigan microwave canopy scattering model. *Int. J. Remote Sens.* **1990**, *11*, 1223–1253.
45. Baghdadi, N.; Le Maire, G.; Bailly, J.S.; Osé, K.; Nouvellon, Y.; Zribi, M.; Lemos, C.; Hakamada, R. Evaluation of ALOS/PALSAR L-band data for the estimation of *Eucalyptus* plantations aboveground biomass in Brazil. *IEEE J. Sel. Top. Appl. Earth Obs. Remote Sens.* **2015**, *8*, 3802–3811.
46. Ulander, L.M.H. Radiometric slope correction of Synthetic-Aperture Radar images. *IEEE Trans. Geosci. Remote Sens.* **1996**, *34*, 1115–1122.
47. Matsumoto, M. Carbon stock and carbon sequestration by the forests of Japan. *Shinrin Kagaku.* **2001**, *33*, 30–36. (In Japanese)
48. Forestry and Forest Products Research Institute. Guidelines for Implementing REDD-plus ver. 1.1. Available online: http://www.ffpri.affrc.go.jp/reddrdc/en/reference/guideline/REDD+Guidelines_E_ver.1.1_20140327.pdf. (accessed on 6 August 2015).